Swansea University
Prifysgol Abertawe

The role of ferroptosis in Tuberous Sclerosis Complex disease

Douglas Furlong

Submitted to Swansea University in fulfilment of the requirements for the degree of Master of Science by Research

Swansea University, 2024

Supervised by Dr James Cronin and Dr Matthew Hitchings.

Abstract

Tuberous Sclerosis Complex disease is a rare genetic disorder that results in the uncontrolled growth of affected cells, leading to the development of benign tumours in different tissues of the body that cause neurological disorders, skin problems, and heart, kidney and lung dysfunction. The condition is characterised by mutations in the TSC subunit genes (*TSC1* or *TSC2*) leading to continuous activation of the mammalian target of rapamycin (mTOR) pathway, a central driver of cell proliferation and metabolism. Rapidly dividing cells require increased iron metabolism to maintain a wide spectrum of cellular processes, such as DNA synthesis and cellular respiration. However, these processes must be tightly regulated as excess iron is toxic to cells, via reactive oxygen species (ROS) and Fenton reactions, triggering ferroptosis, an iron-dependent form of programmed cell death. To avoid ferroptosis, cells must upregulate pathways that detoxify ROS. Tied into this is the role glutathione peroxidase enzymes (GPXs) play in regulating ROS homeostasis. Preliminary data from collaborators shows increased expression of Gpx8 in $TSC2^{-/-}$ mouse embryonic fibroblasts (MEFs). Localised to the endoplasmic reticulum (ER), GPX8 is an enzyme which neutralises the build-up of hydrogen peroxide (H_2O_2), an important ROS involved in lipid peroxidation and the induction of ferroptosis. Furthermore, the overexpression of GPX8 has been shown to be associated with an aggressive phenotype in breast cancer due to its influence on the epithelial-mesenchymal transition required for metastasis (Khatib et al., 2020). We hypothesise that GPX8 plays a role in the evasion of ferroptosis in Tuberous Sclerosis Complex patient tumours.

This project will use RNA-seq data from $TSC^{-/-}$ AML cells to profile genes involved in ferroptosis. We will use $TSC2^{-/-}$ and $TSC2^{+/+}$ (wt) angiomyolipoma (AML) cells derived from Tuberous Sclerosis Complex patient kidneys as a disease model to explore the role GPX8 and ferroptosis play in Tuberous Sclerosis Complex disease. The proteins involved in the induction/evasion of ferroptosis will be explored by immunoblotting, flow cytometry and confocal microscopy. Small molecule inducers of ferroptosis or siRNA targeting of GPX8 expression will be used for viability assays and wound healing assays in $TSC2^{-/-}$ vs wt cells.

Declarations:

This work has not previously been accepted in substance for any degree and is not being concurrently submitted in candidature for any degree.

Signed .... 

Date ……27/09/2024……

Statement 1

This thesis is the result of my own investigations, except where otherwise stated. Where correction services have been used, the extent and nature of the correction is clearly marked in a footnote(s).

Other sources are acknowledged by footnotes giving explicit references. A bibliography is appended.

Signed ..... 

Date ……27/09/2024……

Statement 2

I hereby give consent for my thesis, if accepted, to be available for photocopying and for inter-library loan, and for the title and summary to be made available to outside organisations.

Signed ..... 

Date ……27/09/2024……

Table of contents

List of Abbreviations:

AA: Arachidonic acid
ABAM: Antibiotic-antimycotic
ACSL4: Acyl-coenzyme A synthetase long-chain family member 4
AKT: Protein kinase B
AML: Angiomyolipoma
AMP: Adenosine monophosphate
AMPK: AMP-activated protein kinase
APS: Ammonium persulfate
ATP: Adenosine triphosphate
BSA: Bovine Serum Albumin
CB-839: Telaglenastat
CGGA: Chinese Glioma Genome Atlas
DFO: Deferoxamine
DMEM: Dulbecco's Modified Eagle Medium
DNA: Deoxyribonucleic acid
ECAR: Extracellular acidification rate
EPA: Eicosapentaenoic acid
ER: Endoplasmic reticulum
ETC: Electron transport chain
FBS: Fetal Bovine Serum
FINs: Ferroptosis inducing compounds
FSP1: Ferroptosis suppressor protein 1
FTH1: Ferritin heavy chain 1
GAC: Glutaminase isoform C
GAP: GTPase-activating protein
GDH: Glutamate dehydrogenase
GEPIA: Gene Expression Profiling Interactive Analysis
GLS: Glutaminase
GPX4: Glutathione peroxidase 4
GPX8: Glutathione peroxidase 8
GS: Glutamine synthase
GTP: Guanosine triphosphate
HRP: Horseradish peroxidase
KEAP1: Kelch-like ECH-associated protein 1
KGA: Kidney Glutaminase A
mTORC1: mammalian target of rapamycin complex 1
MTT Assay: 3-(4,5-dimethylthiazol-2-yl)-2,5-diphenyltetrazolium bromide Assay
MUFA: Monounsaturated fatty acid
NRF2: Nuclear factor erythroid 2-related factor 2
OA: Oleic acid
OCR: Oxygen consumption rate
PA: Palmitic acid
PBS: Phosphate Buffered Saline
PM: Plasma membrane
PUFA-PL: Polyunsaturated fatty acid phospholipid
PUFA: Polyunsaturated fatty acid

PVDF: Polyvinylidene fluoride
RNP: Ribonucleoprotein
ROS: Reactive oxygen species
RSL3: RAS-selective lethal 3
SCD1: Stearoyl-CoA desaturase 1
SDS-PAGE: Sodium Dodecyl-sulfate polyacrylamide gel electrophoresis
SEM: Standard error of the mean
shRNA: Short-hairpin ribonucleic acid
siRNA: Small interfering ribonucleic acid
TBST: Tris-buffered saline TWEEN
TCA cycle: Tricarboxylic acid cycle
TCGA: The Cancer Genome Atlas program
TEMED: tetramethylethylenediamine
TIMER2.0: Tumour Immune Estimation Resource
TSC: Tuberous Sclerosis Complex
UFA: Unsaturated fatty acid

Acknowledgements:

This project would not have been possible without the endless support and guidance from Dr James Cronin. A great deal of thanks is also due to all the staff and students on the 2nd and 4th floors of ILS1, with specific mention of Rhiannon Beadman and Emma Stanton who contributed an enormous amount of time in aid of the development of my lab skills.

The CRISPR protocols for this research project were designed and carried out with considerable input and supervision from Dr Fernando Ponce Garcia, Postdoctoral Research Officer at Swansea University.

List of figures:

1. Introduction

1.1 Tuberous Sclerosis Complex disease

Tuberous Sclerosis Complex (TSC) disease is a clinically challenging and potentially debilitating autosomal disorder affecting around 1 in every 6000 births in the USA each year (NINDS, 2023). There is currently no cure for the disease, although several treatments are available for common symptoms (Frost and Hulbert., 2015). Symptoms include seizures, developmental delays, and other neurological difficulties. TSC disease leads to these symptoms through the growth of benign tumours around the body, with tumours in the brain causing the recognisable neurological symptoms. Other common tumour locations include kidney, heart, and skin, all of which produce their own unique complications (Portocarrero et al., 2018). Unfortunately, female patients are also more vulnerable to renal and pulmonary disease than male patients (Amin et al., 2016). Lymphangioleiomyomatosis (LAM) is rare lung disease characterised by the abnormal accumulation of smooth muscle cells (Moss et al., 2001). Sporadic LAM almost exclusively affects female patients, suggesting a strong hormonal link (Darling et al., 2010). LAM is progressive disease, and common symptoms include dyspnoea (the feeling of running out of air) and recurrent pneumothorax (Taveria-DaSilva et al., 2010).

TSC disease garners its name from tuber-like nodules in the brain of a patient from the 19th century with the disease, with the proteins that make up the heterodimer complex subsequently named after this disease. This complex consists of TSC1 and TSC2 proteins, also known as hamartin and tuberin (Feliciano., 2020), and a third core subunit of TBC1D7 that regulates the association of TSC1 and TSC2. Knockdown of TBC1D7 leads to increased mTORC1 signalling, as would be expected of the other parts of the complex. As part of normal cell function, the TSC complex acts as an essential negative regulator of mammalian target of rapamycin complex 1 (mTORC1) through its GTPase-activating protein (GAP) action on the G-protein Rheb, preventing uncontrolled cell growth and proliferation (Huang and Manning., 2008). In disease subjects, loss of function mutations in either protein leads to dysfunction of the complex, and a release of the brake on mTORC1 signalling. In addition to this, without a functioning TSC complex, other negative regulators of cell growth, such as fuel-sensing enzyme AMP-activated protein kinase (AMPK) (Herzig and Shaw., 2018), or hypoxia

(Champion et al., 2022), are ineffective. As such, diseased cells can proliferate uncontrollably and form the tumours representative of TSC disease.

1.2 Tuberous Sclerosis disease presentation

The tumours that arise as a result of the TSC mutation can lead to numerous symptoms, including but not limited to epilepsy, learning disabilities, autism spectrum disorder, skin abnormalities, breathing difficulties, and hydrocephalus (NHS, 2021). Symptoms can express themselves as small inconveniences that go easily unnoticed, to life altering conditions. There is currently no treatment for TSC disease, but the symptoms can be managed by interventions that would be used if these symptoms were a standalone condition.

Symptoms and presentations related to the kidney are a consist problem among those with the disease. Renal angiomyolipomas (AMLs) represent a significant proportion of benign tumours in TSC patients. Presentation of AMLs has been reported in up to 60% of all TSC patients (Nair et al., 2020). Furthermore, renal cysts have been reported in up to 32% of TSC patients which while often without symptoms, can grow large enough to cause pain, kidney failure, and internal bleeding (NIH, 2025). Even in the absence of specific symptoms, AMLs and cysts can reduce renal function. On average, 40% of TSC patients live with reduced renal function even without other serious outcomes or interventions (Kumar et al., 2021).

1.3 Tuberous Sclerosis Disease Treatment

Despite the lack of a universal treatment for TSC disease, there are both promising developments within healthcare as well as more-established practices for the treatment of the common symptoms. As with most diseases involving the development of tumours, surgery is an option but is becoming less favourable overtime compared to medical options (Li et al., 2019). Inhibitors of mTOR, such as rapamycin and its derivative everolimus, have proven clinically promising. Several studies have suggested the ability of these compounds to control tumour growth (Hatano et al., 2019; Trelinska et al., 2015; Cinar et al., 2017), but there are still concerns over the long-term effects and safety of using mTOR inhibitors as a therapeutic option (Li et al., 2019). The FDA currently only approves of the use of everolimus for renal AML and subependymal giant cell astrocytoma (SEGA) (Sasongko et al., 2023). A meta-analysis from the international journal of oncology concluded that despite the

significant prevalence of side effects such as stomatitis, anorexia, and anaemia during treatment with everolimus they were classed as a low enough grade to be easily managed by clinicians (Arena et al., 2021). The Multicentre International LAM Efficacy of Sirolimus (MILES) trial sought to investigate the long-term effects of the 'rapalog' sirolimus in LAM patients. After 5 years, 59% of the treatment group had experienced a positive effect, quantified through measurement of force expiratory volume in 1 second (FEV1) (Revilla-Lopez et al., 2021; McCormack et al., 2011).

In the case of neurological disorders caused by TSC disease, treatment can be both therapeutic and interventional. Antiepileptic drugs such as vigabatrin (Słowińska et al., 2021) resulted in positive outcomes regarding epilepsy outcome and cognitive function. On top of this, early interventions including speech and behavioural therapy can be effective in improving the quality of life for patients. However, it is important to consider that developmental delays will be unique to each individual, thus requiring personalised changes in treatment plans and neurological interventions. Small scale studies on infants with TSC disease have shown promising outcomes following parent-mediated behavioural interventions (McDonald et al., 2020).

TSC disease and ferroptosis have not been strongly linked within published literature, providing an interesting avenue of approach. The uncontrolled proliferation of cells identified as part of TSC disease, and the resulting biochemical consequences, ties in well with the function of ferroptosis as a response to the build-up of reactive oxygen species. We believe ferroptosis provides promise as an area of research that might reveal a universal approach to TSC disease treatment, that is greatly needed by those affected.

1.4 Ferroptosis

Just over a decade after its initial identification by Stockwell and Dixon (Dixon et al., 2012), ferroptosis is an increasingly hot topic in the cancer research space. However, with around 1600 publications within PubMed in 2021 (Stockwell., 2022) ferroptosis trails significantly in research interest and popularity behind other forms of cell death such as apoptosis, which garnered over 38,000 publications in 2021. Along with a select few research groups and institutions, we consider ferroptosis an increasingly exciting and promising area of research with a lot of questions still to be answered.

Ferroptosis is an iron-dependent form of programmed cell death that is distinct from apoptosis and necrosis. It is characterised by the build-up of toxic lipid peroxides within the cell membrane. Ferroptosis can be observed in cells as a reduction in cell volume and increased mitochondrial membrane density alongside disappearance of the cristae (Li et al., 2020). This mechanism of cell death was first characterised in 2012 by Dixon after studying the effects of erastin on cystine/glutamate transport in cancer cells. They coined the term ferroptosis, as the mechanism of cell death was reliant on iron, but not other intracellular metals (Dixon et al., 2012). It was later shown that iron chelators effectively inhibit ferroptosis, cementing the dependence of this form of cell death on intracellular iron (Chen et al., 2020). There are many facets to the induction of ferroptosis, including but not limited to lipid metabolism, iron storage and transport, glutamine metabolism, antioxidant defence, and mitochondrial function.

Ferroptosis can be induced through the use of compounds collectively known as Ferroptosis inducing compounds (FINs)(erastin, RAS-selective lethal 3 (RSL3), and buthionine sulfoximine) some of which are used clinically (sulfasalazine, sorafenib, and artesunate)(Xie et al., 2016). These can be exceptionally useful for ferroptosis research to both guarantee that death is occurring via ferroptosis, as well as investigate compounds that may rescue cells from ferroptosis *in vitro*. The two most frequently used compounds, erastin and RSL3, induce ferroptosis through inhibition of cystine/glutamate transport through system x_c^- and inhibition of antioxidant enzyme GPX4, respectively (Fig. 1).

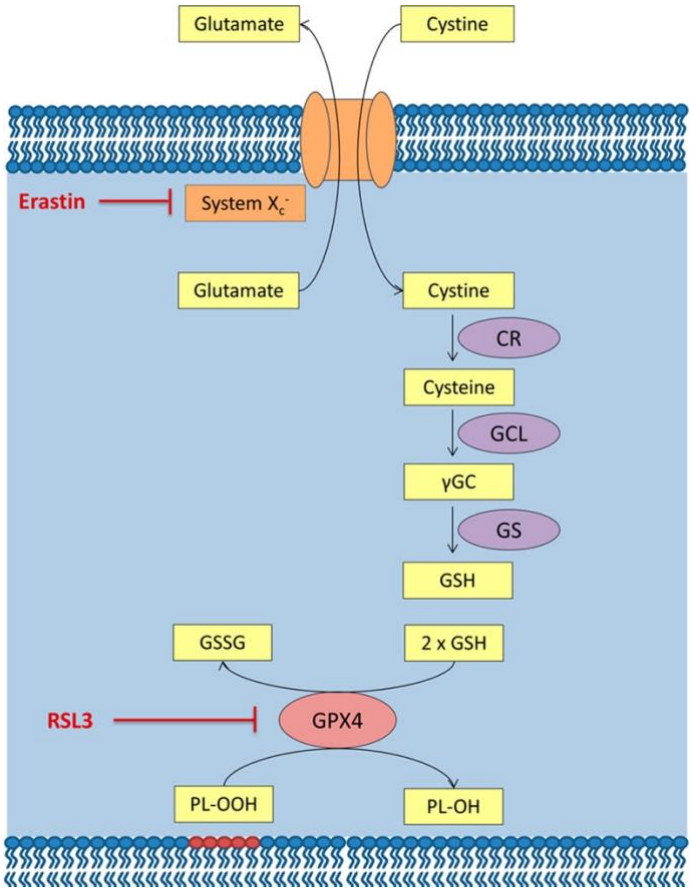

Figure 1: Ferroptosis inducing compounds Erastin and RSL3 and their antioxidant enzyme targets (Devisscher et al., 2018). GPX4 is an enzyme central to the study of ferroptosis and is reliant on this synthesis pathway for its effects. Conversion of cysteine to γGC is the rate limiting step of the pathway. CR – cysteine reductase, GCL – glutamate cysteine ligase, γGC – γ-glutamyl cysteine, GS – glutathione synthase, GSH – glutathione, GSSG – glutathione disulfide, PL-OOH – lipid peroxide, PL-OH – lipid alcohol.

Unlike other forms of cell death, ferroptosis does not require a defined initiator protein to jump start the process (McIlwain et al., 2013; Han et al., 2020). Instead, lipid peroxidation causes sufficient cell membrane damage to perform this function (Stockwell et al., 2017). The required toxic lipid peroxides are a result of reactions involving iron and polyunsaturated fatty acid-phospholipids (PUFA-PL) that cause further oxidation of these lipids. This process depends on the Fenton reaction (Fig. 2), whereby hydrogen peroxide reacts with intracellular ferrous iron (Fe^{2+}) to form hydroxyl radicals which subsequently attack the plasma membrane and trigger lipid peroxidation (Henning et al., 2022). The essential nature of this process to the initiation of ferroptosis can be shown through treatment of ferroptotic cells with iron chelating compounds such as deferoxamine (DFO), which sequesters ferric iron (Fe^{3+}) away

from the cell to be removed as waste by the kidneys, or 2,2'-bipyridine which has an equivalent function for Fe^{2+} (Chen et al., 2020).

The storage and transport of iron within the cell is an essential component of the antioxidant responses of the cell, especially in the context of ferroptosis. *FTH1*, the gene which codes for the heavy chain of iron storage compound ferritin, has its transcription controlled by the KEAP1/NRF2 pathway which senses and responds to oxidative stress within the cell (Lee et al., 2021).

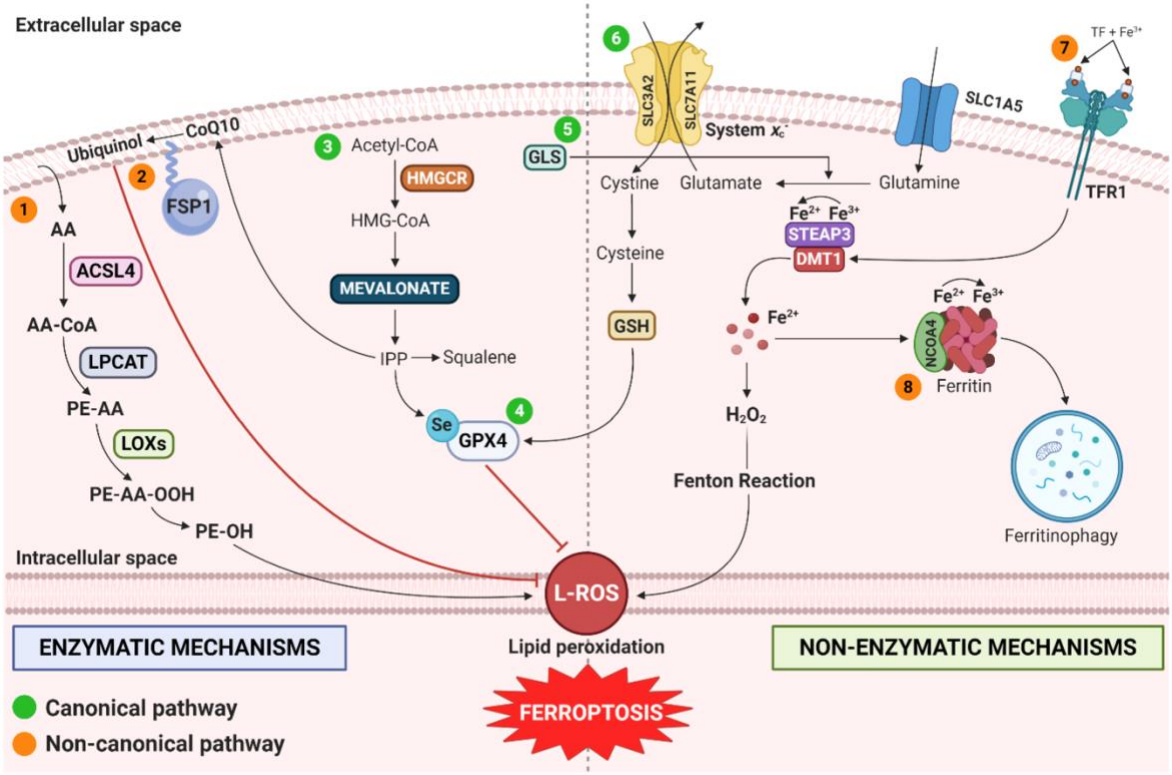

Figure 2: The metabolic pathways contributing to ferroptosis, effectively showing the importance of a variety of inputs to produce lipid peroxides. The Fenton reaction is the main producer of reactive oxygen species that attack the lipid membrane and convert PUFA-PL into lipid peroxides (Battaglia et al., 2020).

The link between ferroptosis and mTORC1 is not currently well defined. Research has shown mTOR having both positive and negative on ferroptosis. For example, mTOR overexpression in mouse cardiomyocytes suppressed erastin and RSL3 induced cell death, with deletion of mTOR having the inverse effect (Baba et al., 2018). Additionally, mTOR inhibition can also

modulate the transport of iron in and out of the cell, consequently modulating ferroptosis through a reduction in iron-dependent oxidative stress (Cosialls et al., 2023). Conversely, specific mTOR inhibitors have been shown to limit ferroptosis that was induced by class 1 FINs such as erastin, but not by RLS3 (Conlon et al., 2021; Lei et al., 2021). On top of this, further investigation suggested that by driving excessive protein synthesis, mTOR hyperactivation was able to reduce the availability of amino acids are required for glutathione synthesis (Conlon et al., 2021; Yu et al., 2016). Overall, there is a significant amount of uncover about the links between mTOR and ferroptosis, and it is important to consider both angles when discussing their roles.

1.5 Lipid Metabolism

Ferroptosis relies on lipid metabolism to enable the resultant lipid peroxidation that characterises this form of cell death. Monounsaturated fatty acids (MUFAs) produced by *de novo* lipogenesis, are less susceptible to lipid peroxidation compared to polyunsaturated fatty acids (PUFAs) (Rodencal and Dixon., 2022). This can be shown through supplementation of MUFAs into cells that have had ferroptosis induced, and the resulting improvement in cell viability (Kim et al., 2023).

The incorporation of PUFAs into cell membranes is one of the hallmarks of lipid metabolism that enables cell death by ferroptosis. PUFAs that are incorporated into plasma membrane lipids are vulnerable to lipid peroxidation due to the presence of bis-allylic sites that can be attacked by reactive oxygen species. MUFAs do not share this susceptibility. Exogenous supplementation of MUFAs, such as oleic-acid (OA) and palmitic acid (PA), promotes a ferroptosis-resistant phenotype in a range of cancer cells (Magtanong et al., 2019). Inversely, supplementation of PUFAs, such as arachidonic acid (AA) and eicosapentaenoic acid (EPA), induces ferroptosis in cancer cells (Magtanong et al., 2019; Krusenstiern et al., 2023).

Ferroptosis can be induced through the lipid peroxidation of all cellular membranes, including the endoplasmic reticulum (ER), mitochondrial membrane, and plasma membrane (PM). It has been shown that lipid peroxidation induced by FINs affects the ER and PM during different time periods, with peroxidation of the ER occurring initially, followed by the PM (von Krusenstiern., et al., 2023). Unfortunately, it is unclear what the final effector of ferroptotic cell death might be, such as that seen in apoptosis (Elmore., 2009). Not all lipid peroxidation leads to cell death, and so it has been hypothesised that an unidentified protein may be

required to cause membrane damage because of lipid peroxidation (Tang et al., 2021). However, the physiological results of lipid peroxidation, such as changes in membrane fluidity and structure, may have an impact on barrier function, leading to further cell damage and death (Liu et al., 2022).

While PUFAs are highly vulnerable to lipid peroxidation, PUFA supplementation alone into cell culture does not induce a great degree of ferroptosis (Gan., 2022). Conversely, enzymes that support the incorporation of PUFAs into cell membranes, such as acyl-coenzyme A synthetase long-chain family member 4 (ACSL4), can encourage cell death by ferroptosis (Mortensen et al., 2023). PUFAs within cell membranes are readily oxidisable by reactive oxygen species (often hydrogen peroxide produced by the Fenton reaction) due the presence of 2 or more carbon-carbon double bonds. Arachidonic acid (20:4) and eicosapentaenoic acid (20:5) are both examples of highly oxidisable PUFAs.

Crucially, fatty acids containing only one carbon-carbon double bond are much less susceptible to oxidative attack than PUFAs. MUFAs have been shown to protect cells from ferroptosis, as demonstrated by Tesfay and colleagues in their study that focused on stearoyl-CoA desaturase 1 (SCD1) (Tesfay et al., 2019). A range of MUFAs have been screened for anti-ferroptosis effects, and it was found that only exogenous MUFAs with a centred carbon-carbon double bond could inhibit ferroptosis (Shan et al., 2023). Furthermore, this study found that suppression of SCD1 activity sensitises cells to lipid peroxidation, and therefore ferroptosis. These findings echo previous research linking MUFAs to the ability of cells to resist ferroptosis. Triple negative breast cancer has been shown to secrete an anti-ferroptotic factor when cultured at high densities *in vitro* (Ackermann et al., 2023). This factor was identified as lipids containing monounsaturated fatty acids (MUFAs) and represents a particularly interesting difference in activity between single-cell and high-density cultures in relation to ferroptosis resistance.

Stearoyl-CoA 9-desaturase (SCD) is an endoplasmic reticulum enzyme that catalyses the rate-limiting step of monounsaturated fatty acid synthesis, as part of the *de novo* lipogenesis pathway. SCD converts stearoyl-CoA (or palmitoyl-CoA) to oleic acid (or palmitic acid) through the insertion of a singular double bond at position 9 of the carbon chain. Both MUFAs, oleic acid and palmitic acid attenuate ferroptosis by being significantly less susceptible to

peroxidation than their equivalent PUFA (Pope and Dixon., 2022). SCD1 has been shown to have heightened expression in various ovarian cancer cell lines, resulting in inhibition of this enzyme having significant effects on both lipid peroxidation and cell death (Tesfay et al., 2019). Increased endogenous production of MUFAs, through overexpression of SCD1, or exogenous supplementation of MUFAs significantly increases cell viability *in vitro* (Shan et al. 2020). As expected, the inverse is also true as inhibition of SCD1 using MF-438 or CAY10566 significantly reduced viability across a variety of cell lines. To confirm their findings, administration of oleic acid (MUFA) and ferrostatin, a well-known ferroptosis inhibitor, were used to successfully rescue cell viability.

1.6 Lipid peroxidation

Whilst PUFAs are the target of lipid peroxidation, they are also an essential nutrient that cannot be synthesised *de novo* by vertebrates, and as such precursor lipids (commonly triacylglycerols) must be acquired through the diet (Liu et al., 2014). Prior to incorporation into cell membranes, shorter chain PUFAs such as linoleic acid (18:2) or α-linoleic acid (18:3) undergo a series or desaturation and elongation steps to produce common PUFAs arachidonic acid and eicosapentaenoic acid. Once present in the cell membranes, these PUFAs can then undergo lipid peroxidation.

The process of lipid peroxidation contains three main steps: initiation, propagation, and termination (Ayala et al., 2014)(Fig. 3). Initiation begins with the formation of a lipid radical (L*) through reaction of a PUFA with a free radical such as hydroxyl (OH*) from the Fenton reaction, or superoxide (O*) from the mitochondria (Yin et al., 2011). The propagation step involves the addition of oxygen to the lipid radical (L*) to generate a peroxyl radical (LOO*). Lipid peroxidation is often a chain reaction, meaning that one oxidised lipid can oxidise another and so on. The peroxyl radical is the key component of this chain reaction characteristic. This is sometimes known as autoxidation and provides the basis as to why MUFAs are less vulnerable than PUFAs to lipid peroxidation. The fewer number of carbon-carbon double bonds in a MUFA increases the bond dissociation enthalpy of the surrounding hydrogen atoms (by approximately 10 kcal/mol) compared to the equivalent PUFA. Therefore, bis-allylic C-H bonds in PUFAs are much more vulnerable (and preferentially abstracted) by the peroxyl radical (Yin et al., 2011). This process of lipid peroxidation is self-propagating and will proceed until the termination step occurs. The termination step requires

the donation of a hydrogen atom to the hydroxyl radical by an exogenous antioxidant (such as GPX4), and produces a lipid alcohol (Feng et al., 2018).

Antioxidant enzymes play a significant role in the protection of cells from ferroptosis, either by directly neutralising the lipid radicals in the case of GPX4 (Forcina and Dixon., 2019), maintaining redox balance by neutralising hydrogen peroxide (e.g. GPX8) (Ramming et al., 2014), or regenerating key lipid radical trapping coenzymes, such as ferroptosis suppressor protein 1 (FSP1) (Doll et al., 2019). Antioxidants and their input on ferroptosis will be covered in more detail in **1.2.10.**

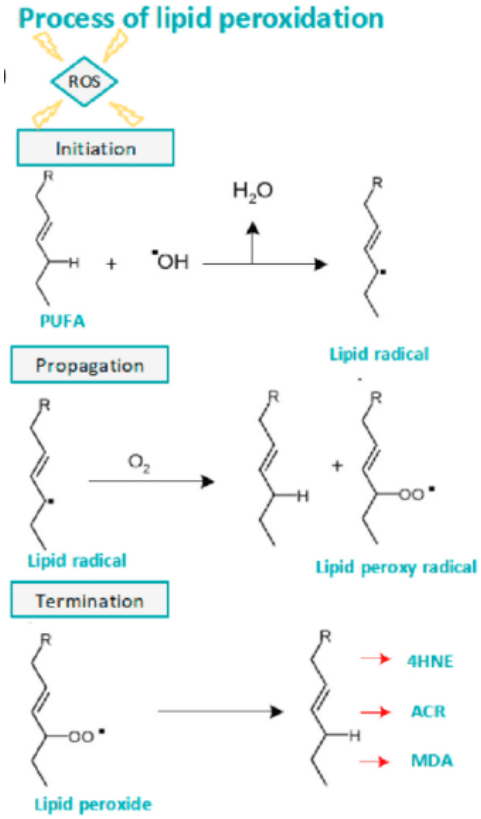

Figure 3: An adapted illustration of the lipid peroxidation cascade (Evans., et al 2021). The three steps of lipid peroxidation: initiation, propagation, and termination. These are initiated by reactive oxygen species (such as produced through the Fenton reaction), but the cycle can be self-sustaining through autoxidation.

1.7 Glutamine Metabolism

Glutamine is a non-essential amino acid that plays an important role in cancer cell metabolism. It can both serve as a carbon source for respiration in rapidly proliferating cells (Kodama et al., 2020) as well as a precursor for important cellular components such as nucleic

acids and proteins (Yoo et al., 2020). Glutamine can be produced in the cell via the glutamine synthesis pathway, catalysed by glutamine synthetase (GS), and imported into the cell through membrane bound transporters SLC1A5, SLC38A1, and SLC6A14 (Jin et al., 2023). mTORC1 active cells, such as in TSC disease, make use of glutamine as a carbon source to sustain the increased energy demands of these cells. In this instance, glutamine is first hydrolysed by glutaminase (GLS) enzymes (GLS1 or GLS2) to produce glutamate and ammonia (Kodama et al., 2020). The glutamate produced by this reaction is then converted to α-ketoglutarate through deamination by glutamate dehydrogenase (GDH)(Fig. 4), which is then used in the tri-carboxylic acid (TCA) cycle to produce adenosine triphosphate (ATP) through the electron transport chain (ETC) (Plaitakis et al., 2017; Jin et al., 2023; Wu et al., 2019). However, this process represents a double-edged sword as a part of metabolism, as this energy production from glutamine also produces reactive oxygen species that can lead to lipid peroxidation.

Glutamine also plays an important role in the antioxidant defences of cells in response to oxidative stressed placed upon rapidly proliferating cells. This aspect of glutamine metabolism is multi-faceted and may provide key avenues of approach in the treatment of TSC disease. To participate in antioxidant defence, glutamine must first be converted to glutamate as described above. Glutamate can then play two distinct roles. Firstly, increased intracellular glutamate enables transport of cystine into the cell via the membrane transporter system x_c^- (Jyotsana et al., 2022). Inside the cell, cystine is reduced to cysteine which is one component, and the rate-limiting step, of glutathione production (Pizzorno., 2014). The remaining components of the tripeptide are glycine, an abundant non-essential amino acid, and glutamate, of which this is its second role in glutathione synthesis.

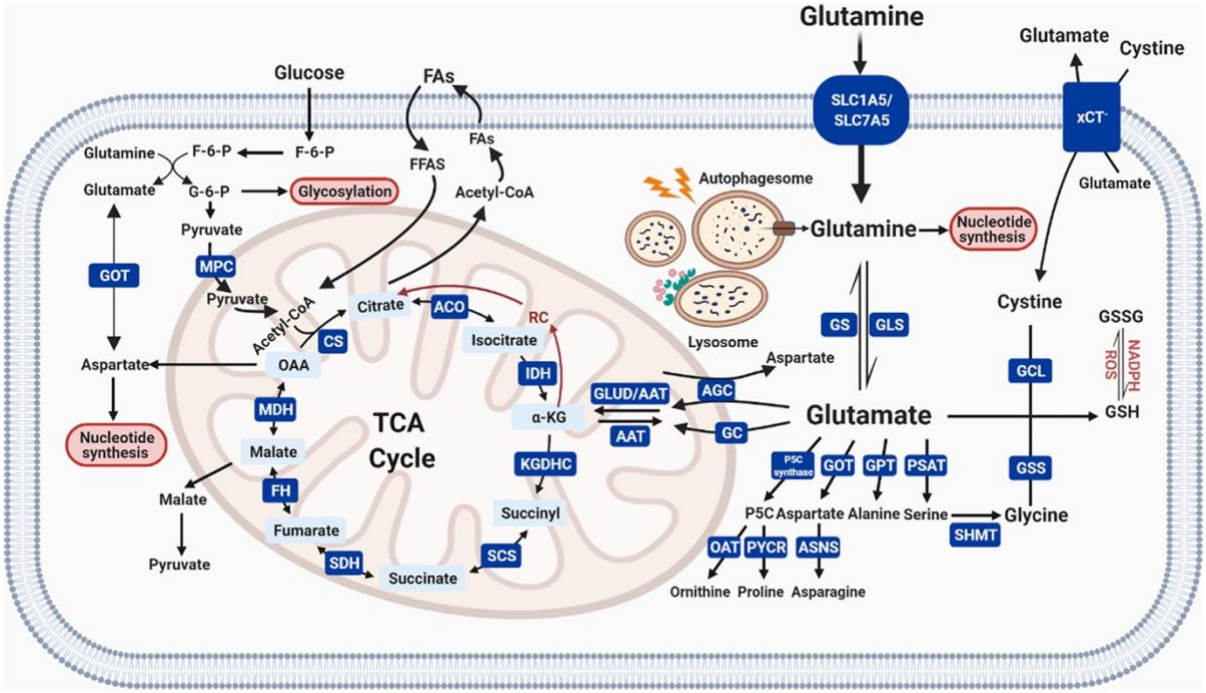

Figure 4: Glutamine metabolism and transport in the cell (Shen et al., 2021). This figure shows in detail the pathway through which cells are able to use glutamine, in particular as a carbon source as part of the TCA cycle. Glutamine can also be used as a part of the synthesis of other amino acids, nucleotides, and fatty acids emphasising the importance of regulation – or advantages of dysregulation – of glutamine availability and metabolism.

1.7.1 Glutaminase enzymes

Glutaminase enzymes catalyse the first step of glutamine metabolism, removing ammonia from glutamine to form glutamate (Yoo et al., 2020). This generates glutamate that enters the mitochondria and acts as a carbon source in the TCA cycle (Guo et al., 2024). As such, glutaminase enzymes have the potential to be key in enabling the uncontrolled growth that we observe in TSC disease and cancer generally. Substrate level phosphorylation can enable the rapid growth and proliferation cancer is known for by meeting the energy demands that glycolysis and oxidative phosphorylation cannot do alone (Seyfried et al., 2010).

Glutaminase is encoded for by two different genes in humans, *GLS1* and *GLS2*. Furthermore, GLS1 has two alternative splice variants, kidney glutaminase A (KGA) and the more active glutaminase isoform C (GAC)(Guo et al., 2024). Colorectal cancer (Turner et al., 2003), cutaneous melanoma (Zacharias et al., 2003), and more recently a range of carcinomas (Xiang et al., 2019) have been shown to have increased expression of glutaminase. The most recent of these studies showing that high GLS1 expression significantly correlated with lymph node

metastasis and the diagnosis of later clinical stages of the disease. CB-839 (Telaglenastat) has recently been the target of several clinical trials (Gross et al., 2014; Jorge., 2023) looking to evaluate its efficacy as a selective and orally bioavailable inhibitor of both splice variants of GLS1. Recently, a small sample size study testing CB-839 in combination therapy with sapanisertib (mTOR inhibitor) finished phase 2 trials and concluded that the combinations lead to tumour shrinkage in the majority of patients and that the treatment was safe and tolerable (Riess et al., 2022). Unfortunately, not all clinical trials have been successful, with a study using a combination of CB-839 and cabozantinib failing to meet its primary end point of increased progression-free survival in patients with advanced renal cell carcinoma (Calithera Biosciences, 2021). As of 2023, clinical trials are being undertaken on CB-839 in combination with a variety of drugs for a range of cancers (Jin et al., 2023).

In contrast to GLS1, GLS2 can act as a tumour suppressor in cancer, enabling ferroptosis through its modulation of glutaminolysis (Suzuki et al., 2022). Increased conversion of glutamine to α-ketoglutarate (α-KG), via GLS2, increases production of lipid reactive oxygen species (ROS) which promote ferroptosis. However, there is substantial evidence that the tumour suppressing capacity of GLS2 is context dependent, and that it can also be pro-tumourigenic in the right circumstances (Buczkowska et al., 2023; Dias et al., 2020). Dias and colleagues showed that in triple-negative breast cancer knockdown of GLS2 decreased cell proliferation, and that GLS2 expression was linked to enhanced migration and invasion.

Compound 968 is another glutaminase inhibitor that recent research has been pinned as a synergistic treatment alongside other therapies (Yuan et al., 2016; Shen et al., 2021; Guo et al., 2023). Compound 968 in combination with paclitaxel was shown to have stronger inhibitory effects on GLS1 than Compound 968 alone, and this inhibition led to cell cycle arrest at G1 and increased ROS production (Guo et al., 2023). This study also linked compound 968 treatment to inhibition of the AKT/mTOR/S6 signalling pathway, which could be especially important in the context of TSC disease.

1.8 Glutamine and ferroptosis

Glutamine is an important metabolic precursor to glutathione (Fig. 5), and therefore essential to the antioxidant defences of the cell. Glutathione acts as a co-factor for the glutathione peroxidase (GPX) family of enzymes which consists of 8 distinct paralogs (Flohe and Brigelius-

Flohe., 2011). Of significant interest in our research are GPX4 and GPX8, as they catalyse separate reactions that both aim to decrease lipid peroxidation in cellular membranes. GPX4 is a selenoprotein that catalyses the conversion of membrane lipid peroxides into non-toxic lipid alcohols and acts as a central regulator of ferroptosis (Yang et al., 2014). Knockdown or inhibition (by RLS3) of GPX4 have been shown to have lethal consequences in a range of cancer cell lines (Yang et al., 2014; Forcina and Dixon., 2019). Interestingly, GPX8 has received significantly less attention and research, and as a result its role in ferroptosis is not completely clear.

SCL7A11 is a cystine/glutamate antiporter that is responsible for providing the cystine required for glutathione synthesis. Heightened expression of this protein is associated with poor prognosis and therapy resistance in cancer (Jyotsana et al., 2022). SLC7A11 makes up one component of the cystine/glutamate transporter system x_c^-, and requires the assistance of heavy chain subunits of SLC3A2 to enable normal function (Koppula et al., 2020). The terms system x_c^- and SLC7A11 are often used interchangeably to refer to this cystine/glutamate transport function. Erastin, a well-studied FIN irreversibly inhibits system x_c^- (Sato et al., 2018) and has been widely used as a model for ferroptosis in cancer cells (Zhao et al., 2020; Yu et al., 2019; Shibata et al., 2019). Glutathione peroxidase enzymes rely on cysteine for their function, suggesting a link between SLC7A11 (as well as other membrane transporters) and the roles that these enzymes play in cell function.

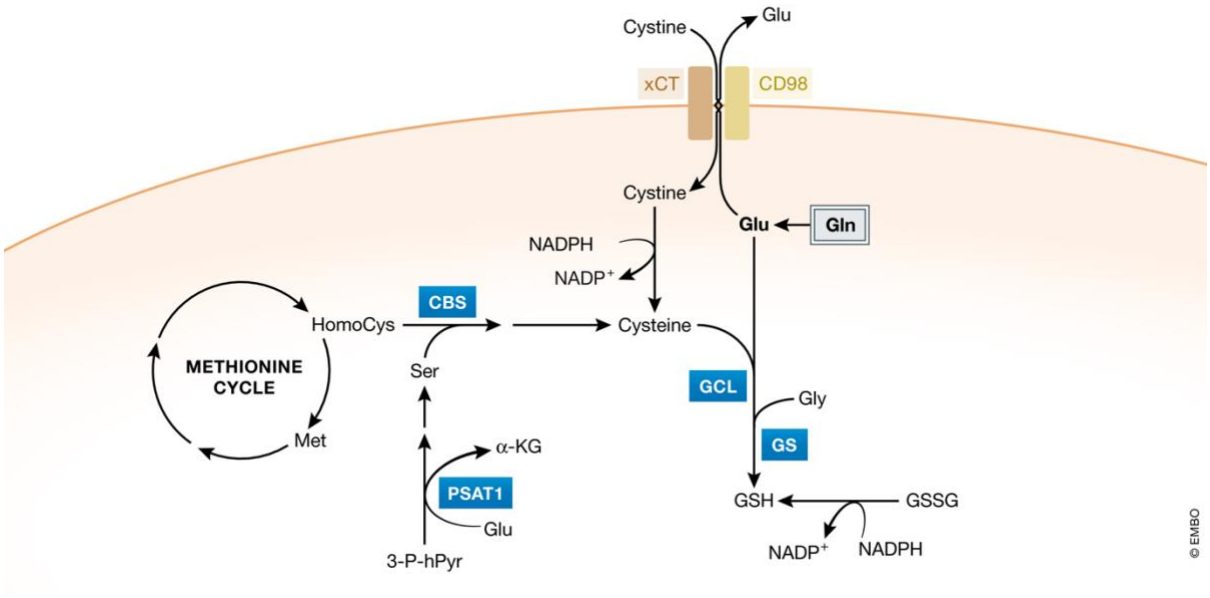

Figure 5: Glutathione synthesis pathway (Zhang et al. 2017). Glutamine-derived glutamate is an essential component in the synthesis of glutathione. Concurrently, glutamate is used in ion exchange to import cystine into the cell, which is converted to cysteine and makes up the second essential component of glutathione synthesis. Gln: glutamine; Glu: glutamate; Gly: glycine; GSH: glutathione; GSSG: glutathione disulfide; α-KG: α-ketoglutarate: Ser: serine; Met: methionine; HomoCys: homocysteine; GCL: glutamate–cysteine ligase; GS: glutathione synthetase; CBS: cystathionine beta-synthase; PSAT1: phosphoserine aminotransferase 1.

1.9 Glutathione peroxidase

Glutathione peroxidases (GPXs) are a family of antioxidant enzymes responsible for preventing free radical formation from hydroperoxides (Flohe et al., 2022). Maintaining cellular redox balance is essential for cell survival, especially in the context of ferroptosis where cell death relies on lipid peroxidation (Dixon et al., 2012), and in TSC disease which is characterised by uninhibited cell growth and proliferation (Huang et al., 2008). GPX1 was the first member of the family to be described in 1957 (Mills et al., 1957), with its dependence on selenium as part of its catalytic triad reported later in 1973 (Rotruck et al., 1973). Since these publications, the family has grown to eight enzymes with unique structures and functions (Pei et al., 2023).

Glutathione peroxidase 8 is the GPX that we are most interested in as part of our research. Contrarily to other GPXs, it does not have selenium cysteine as part of its active site but maintains its importance of playing a role in redox balance. Specifically, GPX8 prevents

leakage of H_2O_2 from the endoplasmic reticulum (Ramming et al., 2014; Chen et al., 2023). It has also been found that GPX8 can influence the aggressiveness of breast cancer. A study published in PNAS found that GPX8 expression strongly correlated with various mesenchymal markers, and poor prognoses (Khatib et al., 2020). This is linked to the epithelial-mesenchymal transition, responsible for cancer metastasis. These findings were also corroborated by a more recent paper which used GPX8 expression data sourced from various databases (TCGA, CGGA, GEPIA, and TIMER2.0) to show that GPX8 is a key factor in the prognosis of glioblastoma patients (Li et al., 2022).

In collaboration with Professor Andrew Tee in Cardiff University, RNA sequencing demonstrated that GPX8 was found to be significantly upregulated in $TSC2^{-/-}$ AML cells compared to AML cells where functional TSC2 had been reintroduced. We hypothesise that GPX8 may help to maintain the cells' ability to rapidly grow and proliferate, by neutralising some of the damaging by-products of mitochondrial respiration, such as H_2O_2.

1.10 Hypothesis

We primarily hypothesise that TSC disease cells evade ferroptosis through altered expression of antioxidant enzymes and their required cofactors. Additionally, we theorise that there is a link between glutaminase enzymes and the glutathione peroxidase enzyme family, specifically GPX8. This is due to the possibility of changes in the availability of glutamine following glutaminase treatment.

1.11 Aims and Objectives

Aims

This project aims to provide a link between TSC disease and ferroptosis through various genes, enzymes, and mechanisms that have been associated with glutamine metabolism and ferroptosis.

Objectives

- Analyse RNA sequencing data to guide investigation into the determinants of TSC disease.

- Explore the response of $TSC2^{-/-}$ and $TSC2^{+/+}$ cells after exposure to known ferroptosis inducing compounds (RSL3, Erastin), and glutaminase inhibitors (CB-839, Compound 968).

- Link stearoyl-CoA desaturase (SCD) to TSC disease as this may be a pivotal enzyme in the evasion of ferroptosis.

- Explore the role of antioxidant enzyme GPX8 in the context of glutamine metabolism and ferroptosis.

- Use small interfering RNA and CRISPR gene editing technology to manipulate gene expression in $TSC2^{-/-}$ and $TSC2^{+/+}$ cells and investigate the effects.

- Analyse RNA sequencing data to guide investigation into the determinants of TSC disease.

2. Methods

2.1 Cell culture

Two cell lines were used for this research project; TRI102 are $TSC2^{-/-}$, derived from human kidney angiomyolipoma (AML)(Yu et al., 2004; Goncalves et al., 2017), while TRI103 has the *TSC2* gene re-expressed to represent a non-diseased state. The original publication that developed the method for and the use of TSC-deficient AML cells was published in 2004 for the purposes of investigating lympangioleiomyomatosis (LAM). The tissue used was donated by those with TSC disease and contained mutations in both alleles of TSC2. They hypothesised that due to the intense similarity between the tissues of the two cell lines, that LAM may be a result of AML metastasis (Yu et al., 2004). This was followed up in 2008 with research that successfully re-expressed the TSC2 in these cells, providing an effective representation of the non-diseased state (Hong et al., 2008).

TRI102 ($TSC2^{-/-}$) and TRI103 ($TSC2^{+/+}$) cells were cultured in DMEM media (Thermo Fisher, #41966-029) supplemented with 15% fetal bovine serum (FBS) (Biosera, #FB-1001/500) and 1% antibiotic-antimycotic (ABAM)(Thermo Fisher, #15240096). Cells were maintained in an incubator at 37°C and 5% CO_2.

Cells were passaged every 2 days, depending on the level of confluency. Media was aspirated and disposed of in Virkon (SLS, #CLE1554). The attached cell layer in the T75 flask was then washed gently with approximately 5 ml of phosphate buffered saline (PBS)(Thermo Fisher, #10010023), and the PBS was gently aspirated and discarded. Approximately 2 ml of cell dissociation product, TrypLE Express (Thermo FIsher, #12605010), was added to the flask to detach the cells. The flasks were returned to the incubator for 5 min at 37°C, or until the cell layer had visibly detached from the surface of the flask. Then, 8 ml of complete media was added to the flask to create 10 ml of cell suspension and inhibit the effects of the cell dissociation product through presence of FBS in the media. Depending on the observed confluency of the flask, an appropriate amount of this cell suspension (often >50%) was discarded, and the flask topped up to 20 ml with complete media. All flasks containing cells were returned to 37°C, 5% CO_2 incubators.

2.2 Cell Seeding

To count cells in suspension the Countess 3 Automated Cell Counter (Invitrogen, #16832556) was used with corresponding Countess Cell Counting Chamber Slides (Thermo Fisher, #C10228). A 10 µL sample of cell suspension was taken and mixed in a 1:1 ratio with Trypan Blue (Merck, #T8154-20ML), and 10 µL added to the cell counting slide. The slide was then inserted into the automated cell counter and the number of cells in suspension recorded.

2.3 *3-(4,5-dimethylthiazol-2-yl)-2,5-diphenyltetrazolium bromide* (MTT) Assay

Cells were seeded at a density of $2.5x10^4$ cells/ml in 100 µL of media in each well of a 96 well plate (Thermo Fisher, #10418623). After 24 hours, the media was aspirated and replaced with the relevant treatment media as detailed in *Results*. Following treatment, the media was aspirated and replaced with 100 µL per well media containing 0.5 mg/ml MTT solution (Invitrogen, #M6494). The plates were then incubated at 37°C for 1 hour to allow time for the formazan crystals to form. Once the incubation was finished, the media was gently aspirated and the formazan crystals were solubilised in 100 µL of DMSO per well and the plate incubated at room temperature for 10 min. Absorbance at 570 nm was measured using the FLUOstar Omega Microplate reader (BMG Labtech). If a specific protocol involved the use of CB-839 or Compound 968 pre-treatments, these were added and incubated for 30 minutes, before subsequently adding any ferroptosis inducing compounds. Ferroptosis inducing compounds were diluted in complete media prior to addition to the plate. Any wells that were designated as 'vehicle' included the appropriate concentration of DMSO, as to be comparable to the treated wells.

2.4 Western blot analysis

2.4.1 Protein extraction

Cells were seeded in a 6 well plate (Corning Costar, #10578911) using 3 ml of a cell suspension containing approximately $5x10^4$ cells/ml. After 24 hours of incubation at 37°C and 5% CO_2 the media was aspirated, replaced with treatment media and returned to the incubator. Following treatment, the media was removed from each well and the cells were gently

washed with PBS to remove any excess media containing FBS that may impact protein extraction. Then, 100 µL of Phosphosafe extraction reagent (Merck, #71296) was added to each well to detach and lyse the cells, followed by scraping of the well. The resulting liquid sample was transferred to an appropriate Eppendorf tube and centrifuged at 200 x g for 5 min before being stored at -20°C.

2.4.2 Detergent Compatible Protein Assay

To determine the concentration of protein in the obtained supernatants from **2.4.1** we performed DC assays. For this, 5 µL of samples or protein standards were loaded into a 96-well plate in duplicate. Then 25 µL of 50:1 mixture of reagents A and S (Bio-Rad, #5000113, and #5000115) followed by 200 µL of reagent B (Bio-Rad, #5000114) were added to each well. The absorbance was then measured at 750nm using the FLUOstar Omega Microplate Reader (BMG Labtech). A standard curve was produced using the absorbance values against the known concentrations of the protein standards.

This standard curve was used to determine the volume of protein extraction sample required to yield 20 µg of protein.

2.4.3 Protein separation by SDS-PAGE

The gels used for polyacrylamide gel electrophoresis (PAGE) were hand cast following Bio-Rad guidelines. The reagents required are as follows; separating buffer (#1185-53-1, Melford, UK), stacking buffer (#7732-18-5, Melford, UK), 30% bis-acrylamide (#161014, Bio-Rad, UK); ammonium persulfate (APS) (#A3678, Sigma, UK), and tetramethylethylenediamine (TEMED) (#T9281, Sigma-Aldrich, UK).

To produce four 10% gels, 10 ml of Separating Buffer, 13.2 ml of 30% bis-acrylamide, 40 µl of TEMED, 400 µl of 10% APS and 16.8 ml of distilled water were added to a small beaker. The solution was then syringed between the plates of the assembled casting apparatus until it was filled appropriately. Before the gel was able to set, a small volume of isopropanol (#I9516, Sigma-Aldrich, UK) was added across the top of the gel to help create a smooth and level surface. The gel was left to set for approximately 45 min. Once set, the isopropanol was

poured away. The stacking gel was then added on top of the separating gel. To make enough solution for four stacking gels, 3 ml of stacking buffer, 2 ml of bis-acrylamide, 40 µl of TEMED, 200 µl of APS, and 7ml of distilled water, were added to a small beaker. This solution was similarly syringed between the glass plates of the apparatus to completely fill the glass plates. A 10-well or 15-well comb was immediately inserted into the top of the gel and the gel was allowed to set for 45 min.

To perform SDS-PAGE the gels were assembled into the PAGE tank and filled with running buffer. Samples containing equal parts 2X Laemmli buffer (Merck, #S3401-10VL) and 20 µg of protein sample (according to values determined in **2.4.2)** were heated to 95°C for 5 min using a T100 thermal cycler (Bio-Rad, #1861096) before being loaded into the wells of the gel. As a guide, the first and last wells of the gel contained dual-colour protein ladder (Abcam, ab116028). To separate the loaded proteins, the gel was run at 120V for approximately 60 min.

2.4.4 Protein Transfer

Following the completion of SDS-PAGE, the acrylamide gel was carefully removed from the apparatus and assembled into the 'transfer sandwich' using filters and PVDF membranes (Merck, IEVH08100). The transfer sandwich was placed into the Transblot Turbo Transfer System (Bio-Rad, #1704150) and proteins transferred at 25V for 30 min.

2.4.5 Imaging

PVDF membranes were placed in blocking buffer composed of 5% bovine serum albumin (BSA) in tris-buffered saline/TWEEN (TBST)(150mM NaCl, 50mM Tris-HCl, pH 7.6, 0.1% TWEEN). The membranes were incubated at room temperature, on a gyro-rocker, for 60 min. After blocking, the BSA/TBST was removed, and the membranes were washed three times with TBST. Primary antibodies were diluted according to the manufacturer's instructions and the antibody solution added onto the membranes. The membranes were incubated in the cold room on a gyro rocker overnight. Membranes were then washed three times using TBST before addition of 1:500 dilution of HRP secondary antibody (Cell Signalling Technology, #7074) in BSA/TBST. The membranes were incubated in HRP secondary antibody for 90 min

at room temperature, on a gyro-rocker. Membranes were imaged using the ChemiDoc MP imaging system (Bio-Rad).

2.5 Extracellular glutamate assay

The extracellular glutamate assay (Abcam, #ab138883) was performed on cell supernatants, according to the protocol provided by the manufacturer. The plate was read at Ex/Em = 540/590nm, using the FLUOstar Omega microplate reader (BMG Labtech).

2.6 Seahorse metabolic analysis

To analyse the metabolic properties of our cells, we used the Seahorse XF Pro Analyser (Agilent Systems) to measure extracellular acidification rate (ECAR) and oxygen consumption rate (OCR), and changes to these values under specific conditions. The day prior to the assay, a seahorse XF cartridge was hydrated in an incubator at 37°C, without CO_2 supplementation, using Seahorse XF calibrant buffer (103059-000, Agilent).

Cells were seeded using 80 µL of a $2x10^5$ cells/ml solution to achieve approximately 16,000 cells per well and the plate incubated for 24 hours at 37°C and 5% CO_2. The next day, media was carefully removed from each well taking care not to disturb the cells at the bottom of the well. The wells were gently washed 3 times with specialist DMEM seahorse media without bicarbonate or phenol red (Agilent, #103575-100). After the third wash, the 180 µl of media was left on the cells and the plate was placed in a 37°C incubator without CO_2 supplementation. The required inhibitors (Oligomycin, FCCP, and Rotenone) were made up to the specified concentrations (5 µM, 1.25 µM, and 5 µM respectively) in Seahorse media according to the Seahorse Mito Stress Test user guide (Kit 103015-100, Agilent Systems) and then loaded into the hydrated Seahorse XF cartridge ready for use.

The *Wave* software on the Seahorse XF Pro was used to design experiments, data was analysed using Prism GraphPad software.

2.7 CRISPR-Cas9 Gene Editing

2.7.1 Reagent Preparation

CrRNA (Alt-R® CRISPR-Cas9 crRNA, Integrated DNA Technologies) and tracrRNA (Alt-R® CRISPR-Cas9 tracrRNA, Integrated DNA Technologies) were both resuspended in nuclease-free duplex buffer (#11-05-01-12, Integrated DNA Technologies) to a concentration of 200 µM and stored at –20°C until needed. Duplex RNA to be used for transfection was made by combining a 1:1 ratio of crRNA and tracrRNA in a sterile Eppendorf, followed by being heated to 95°C for 5 min to anneal the RNA.

Immediately before use, the ribonucleoprotein (RNP) complexes were prepared. Duplex RNA was mixed with Cas9 Nuclease (Alt-R™ S.p. Cas9 Nuclease, Integrated DNA Technologies) in a 3:1 ratio, to achieve a 180 pmol final concentration (180 pmol duplex RNA mixed with 60 pmol Cas9 nuclease). If using multiple crRNA guides, as we did, the amount added to the RNP complex was adjusted to maintain the final concentration of 180 pmol. This mixture was left to incubate at room temperature for 15 min to allow the RNP complex to form. After 15 min, the Eppendorf tube was left on ice until the cells were ready for transfection.

2.7.2 Cell transfection

TRI102 and TRI103 cells were cultured as described in **1.1,** counted, and diluted to a concentration of $1x10^6$ cells/ml. $2x10^6$ cells were resuspended in 18 µL of P4 buffer and mixed with 2 µL of a chosen RNP complex created previously (in our case either *GPX8* or *GLS2*). As quickly as possible, this mixture was added to the well of a 16-well 4D-nucleocuvette strip (#V4XP-3032, Lonza Bioscience) and transfected using the EH115 program code on the nucleofector unit (#AAF-1003X, Lonza Bioscience). To continue culture of the transfected cells, 100 µL of pre-warmed media was added to each well used, and the cells were transferred to 24-well plates. Following normal cell culture procedures, the cells were allowed to grow sufficiently before being moved to 6-well plates, and eventually to T25 cell culture flasks. Knockout success was determined by western blotting.

2.7.3 Single cell isolation

Following transfection, cells that had been successfully genetically altered needed to be isolated from cells that continued to express the target gene. To do this, a serial dilution was performed using the transfected and counted cells, down to approximately 150 cells per ml of media. Then, 100 µL of this cell suspension was then seeded into each well of column 1 of a 96 well plate. The remaining wells in the plate were filled with 50 µL of DMEM media ready for serial dilution. To achieve single cells per well, 50 µL of cell suspension was aspirated from Column 1 of the plate and dispensed into Column 2. The suspension was mixed gently inside the well of column 2, before repeating this process with Columns 3 and so on until column 12. The plate was then placed in an incubator at 37°C and 5% CO_2.

Single cells took up to 3 weeks to appear as suitable colonies. These colonies were then scaled up and assessed for knockdown of relevant genes by Western blotting.

2.8 RNA Sequencing

Differentially expressed gene (DEG) analysis of $TSC2^{-/-}$ and $TSC2^{+/+}$ cells samples was carried out as part of research undertaken by the research group lead by Professor Andrew Tee at Cardiff University. Each cell line was prepared in the Tee lab, with library preparation, RNA sequencing, and DEG analysis undertaken by the Wales Gene Park.

Each cell line was cultured according to section **2.1**. The cells were then washed in PBS before lysis with RNAprotect cell reagent (#76104, Qiagen). Lysates were homogenised using Qiashredders (#79656, Qiagen) and RNA was purified from homogenised lysates. Before sequencing, isolated RNA integrity and concentration was determined by Wales Gene Park using an Agilent 4200 TapeStation (G2991BA, Agilent) and RNA screenTapes (5067-5579, Agilent) (Champion., 2023).

Library preparation and RNA sequencing were undertaken following Wales Gene Park protocols, using the NovaSeq6000 referencing system from Illumina. Quality control was performed using FastQC, with the final DEG analysis completed using the DEseq2 package on the R statistics software.

The data set used for this research contained 6 replicates of both $TSC2^{-/-}$ and $TSC2^{+/+}$ cells from which base means, log_2fold change, and adjusted p-values were calculated to be used in the graphical presentation of these results.

2.9 Statistical Analysis

Statistical analysis was performed using the *Prism GraphPad* software (Version 10). Significance was considered as any p-value < 0.05, inclusive of post-hoc testing. In experiments with just two experimental groups, a one-way ANOVA was used to compare means. In experiments with more than two experimental groups, a two-way ANOVA was used. In terms of post-hoc testing, Tukey's Honestly Significant Difference (HSD) test was used when it was necessary to compare all possible pairs of means, while Dunnett's test was used to compare treatment groups to a single control group.

3. Results

3.1 RNA-sequencing analysis of $TSC2^{-/-}$ and $TSC2^{+/+}$ cells

RNA sequencing was carried out on TRI102 ($TSC2^{-/-}$) and TRI103 ($TSC2^{-/-}$) cells to compare the expression of genes between diseased and wild-type ($TSC2^{+/+}$ re-expressed) cells. RNA sequencing was carried out by collaborators at Cardiff University and analysed at Swansea University Medical School with the help of Dr Matthew Hitchings.

Differentially expressed genes (DEGs) were deemed to be significantly up- or down-regulated if they surpassed the threshold of log_2fold change of >1.5, and an adjusted p-value of <0.05. A negative log_2fold change value indicated that the gene was upregulated in the $TSC2^{-/-}$ samples when compared to the $TSC2^{+/+}$ cells. Three DEGs, of particular interest to this research were, *GLS2*, *GPX8*, and *SLC7A11*, as they have potential roles in ferroptosis. *GPX8* and *SCL7A11* are involved in the antioxidant response of the cell, and are upregulated in $TSC2^{-/-}$ cells, while *GLS2*, involved in glutamine metabolism and potentially ferroptosis, is down regulated in $TSC2^{-/-}$ cells, when compared to $TSC2^{+/+}$.

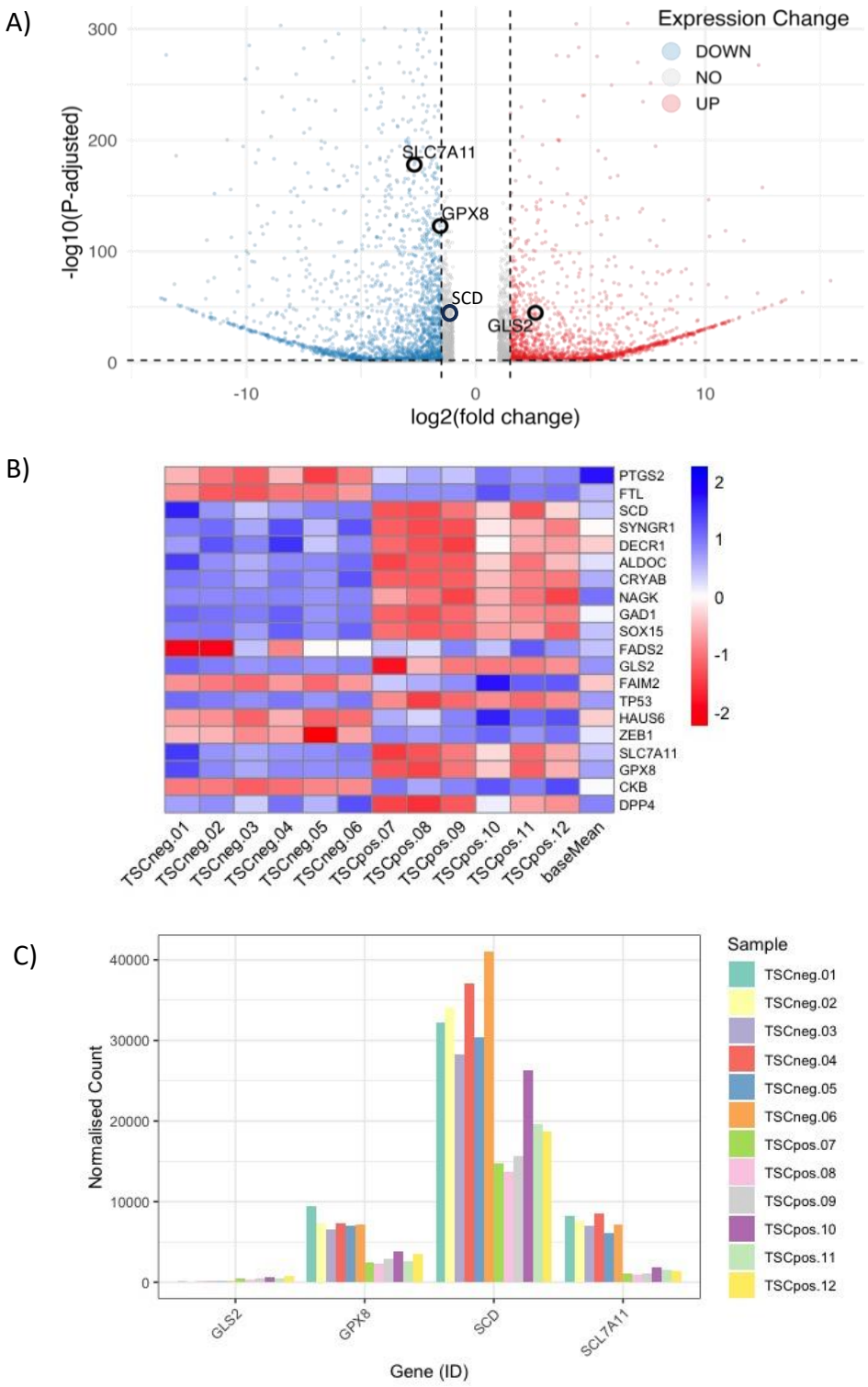

Figure 6: A) Volcano plot comparing gene expression between TSC2$^{+/+}$ and TSC2$^{-/-}$ cells. Positive values represent a gene that is expressed more highly in TSC2$^{+/+}$. Thresholds were defined as a log$_2$ fold change > 1.5, and adjusted p-value < 0.001, and the plot produced using Deseq2 in 'R'. B) Heatmap showing a range of genes associated with ferroptosis and glutamine metabolism. Generated using the "pheatmap' package in R studio, with colour determined by log2 transformation. C) Normalised read counts for the genes highlighted in the volcano plot. Note: GLS2 data is present for TSC negative samples, despite being comparably low.

CRISPR-Cas9 knockout of two DEGs, *GLS2* and *GPX8,* and subsequent western blot analysis highlighted the findings of the RNAseq analysis. For *GPX8*, there appears to be slightly higher expression in the $TSC2^{-/-}$ (TRI102) cells compared to the $TSC2^{+/+}$ (TRI103) cells. *GPX8* was successfully knocked out of both clones and both cell types. Blots for *GLS2* told a different story with significantly higher expression in the $TSC2^{+/+}$ cells compared to the $TSC2^{-/-}$ cells, which matches up well with the results of RNAseq analysis. Once again, *GLS2* was successfully knocked out of both cell lines using CRISPR-Cas9.

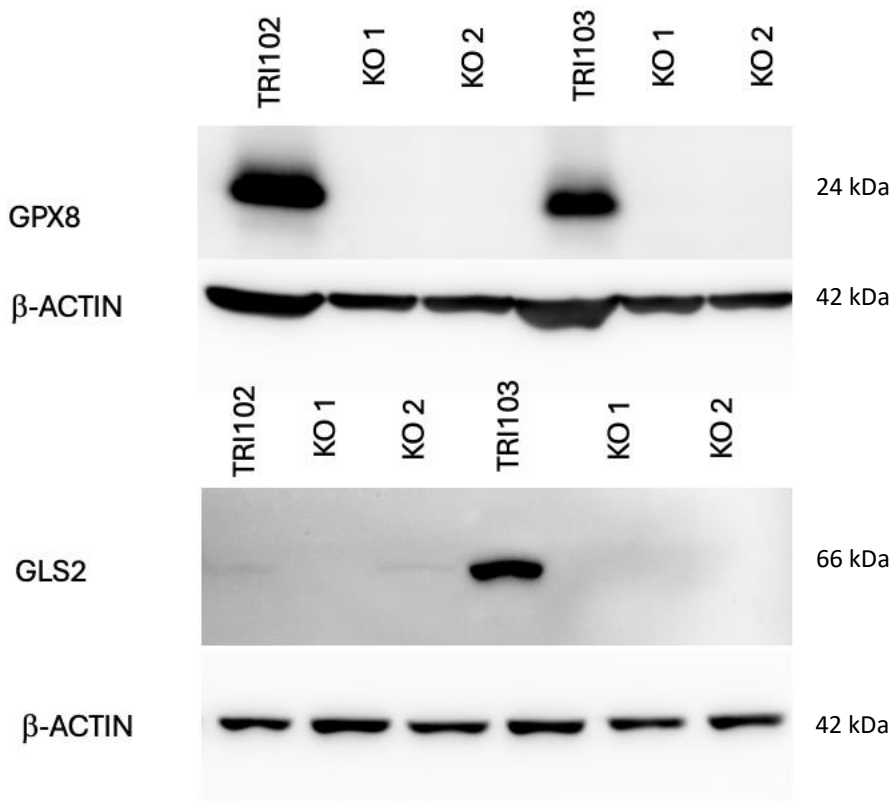

Figure 7: Western blot analysis comparing the expression of key differentially expressed genes (DEGs) GLS2 and GPX8 between $TSC2^{+/+}$ and $TSC2^{-/-}$ cell types, and the effect of CRISPR-Cas9 knockout on this expression.

3.2 Tuberous Sclerosis Complex (TSC2) mutation does not have a significant impact on the sensitivity to RSL3 induced ferroptosis

To determine any differences between *TSC2*$^{-/-}$ and *TSC2*$^{+/+}$ re-expressed AML cells and their sensitivity to ferroptosis, cells were treated with RSL3 at concentrations ranging from 0.15-2.5 µM for 24 h and assayed by MTT. There were no significant differences in susceptibility to ferroptosis observed between the two cell types. All concentrations of RSL3 caused statistically significant decreases in absorbance when compared to vehicle.

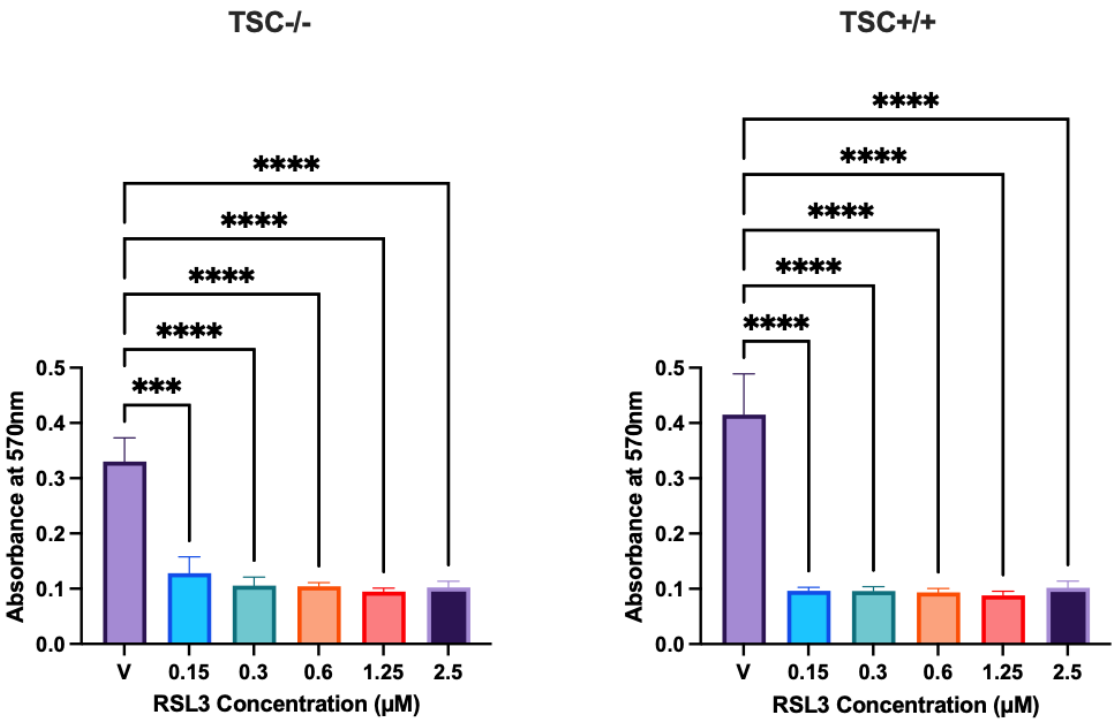

Figure 8: Effect of RSL3 on cell viability on TRI102 (TSC2$^{-/-}$*) or TRI103 (TSC2*$^{+/+}$*) cells. Viability was determined using an MTT assay, measuring the absorbance at 570 nm 24-hours post RSL3 treatment. Data is presented as mean values from three independent cell passage experiments, with the standard error of the mean (SEM) indicated by error bars. Statistical analysis was performed via one-way ANOVA and corrected for multiple comparison using Dunnett's test;* $^{***}P < 0.001$.

3.3 Inhibition of GLS2, but not GLS1, promotes rescue from ferroptosis in TRI102 angiomyolipoma (TSC2$^{-/-}$) cells

The process of cell death by ferroptosis can be strongly linked to amino acid metabolism. Amino acids, specifically glutamine, can be linked to both the induction of ferroptotic cell

death (Ye et al., 2024) and its evasion (Li et al., 2022). To investigate the role of glutamine metabolism and ferroptosis in TSC disease, TRI102 ($TSC2^{-/-}$) and TRI103 ($TSC2^{+/+}$) angiomyolipoma cells were pre-treated with 10 µM of either CB-839 (purported GLS1 inhibitor (Gross et al., 2014) or Compound 968 (purported GLS1/GLS2 inhibitor) (Lukey et al., 2019; Shen et al., 2021). Pre-treatment with the GLS1 inhibitor CB-839 showed no significant effect on cell viability in either $TSC2^{-/-}$ or $TSC2^{+/+}$ cells. Although, there was a reduced trend for the $TSC2^{+/+}$ cells. Furthermore, CB-839 did not affect the reduction in cell viability at any concentration of RSL3 (Fig. 9).

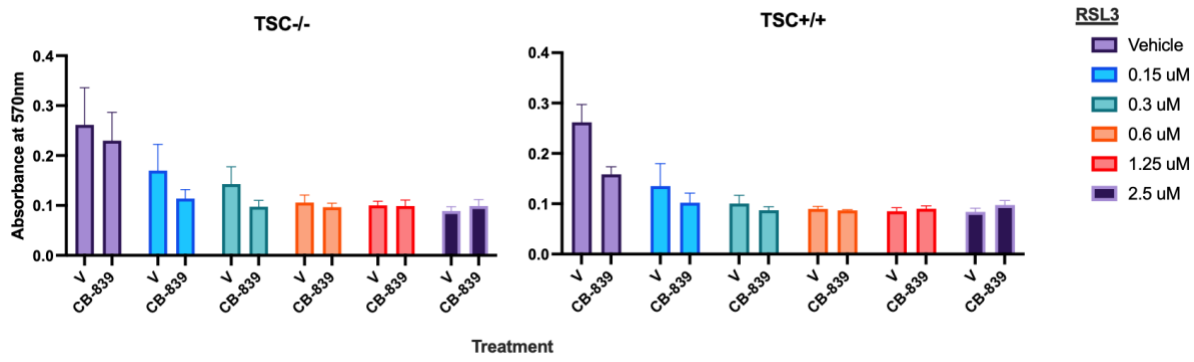

Figure 9: Effect of RSL3 on cell viability following pre-treatment with GLS1 inhibitor CB-839 (10 µM). *Absorbance measurements were produced using MTT assay after 24 hours of incubation. Data is presented as mean values from three independent cell passage experiments, with the standard error of the mean (SEM) indicated by error bars. Statistical analysis was performed via Two-Way ANOVA.*

Pre-treatment of cells with GLS1/GLS2 inhibitor compound 968 alone showed no effect on cell viability; however, compound 968 was shown to rescue the $TSC2^{-/-}$ cells from RSL3 induced death at all concentrations. In comparison, although there was a trend, compound 968 did not result in statistically significant rescue at any concentration of RSL3 in the $TSC2^{+/+}$ cells (Fig. 10). These data suggest that GLS2 may contribute to driving ferroptosis in $TSC2^{-/-}$ cells. As shown in section **3.1**, GLS2 is downregulated in $TSC2^{-/-}$ cells and when taken into consideration with the findings presented here, suggest that the effects produced by Compound 968 treatment may be independent of its reported GLS1/GLS2 inhibition.

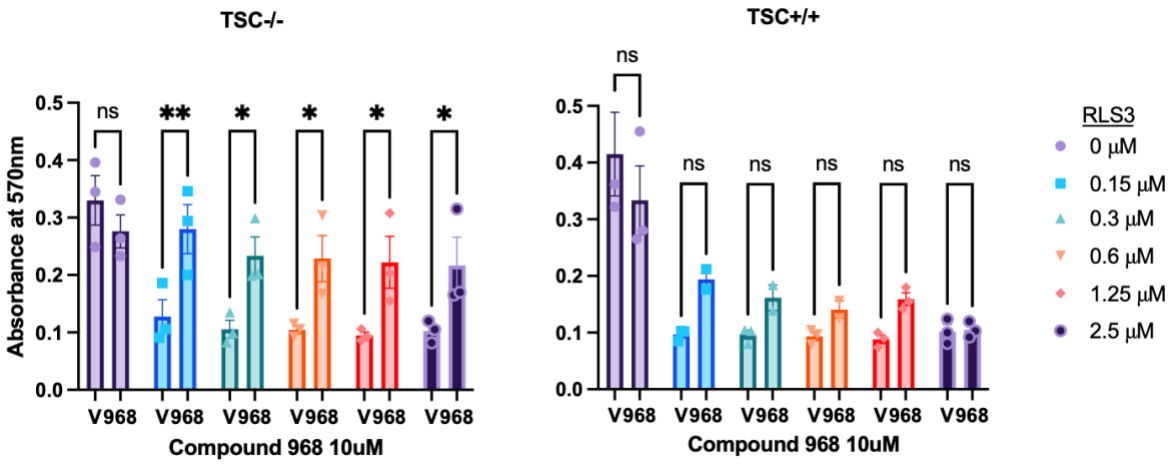

Figure 10: Effect of RSL3 on cell viability following pre-treatment with GLS1/GLS2 inhibitor Compound 968 (10 µM*). Absorbance measurements were produced using MTT assay after 24 h of incubation. Data is presented as mean values from three independent cell passage experiments, with the standard error of the mean (SEM) indicated by error bars. Statistical analysis was performed via Two-Way ANOVA, followed by Tukey's post-hoc test for multiple comparisons;* $^{*}P < 0.05$; $^{**}P < 0.01$.

3.4 Glutamine starvation influences compound 968 mediated rescue

To further understand the role of glutamine in compound 968 mediated cell viability rescue, we simulated reduced glutamine availability by treating cell samples in media containing 2 mM (normal) or 0.2 mM (starved) glutamine. Other than glutamine, the formulation of each media was identical. The final concentrations of the inhibitors were 0.15 µM for RSL3, and 10 µM for Compound 968 or CB-839. For $TSC2^{-/-}$ and $TSC2^{+/+}$ cells, glutamine starvation led to a significant decrease in cell viability measured by MTT assay (Fig. 11) Importantly however, this did not affect the pattern of results seen previously in the $TSC2^{-/-}$ cells, while the $TSC2^{+/+}$ cells lost the moderate rescue effect caused by compound 968 when starved of glutamine (Fig. 11). From these data we can suggest that glutamine is a factor in the viability of both cell types. On top of this, the data shows that compound 968 has an increased effect on $TSC2^{-/-}$ cells. Inhibition of GLS1/GLS2 by Compound 968 increasing cell viability echoes the findings of our RNAseq analysis, that shows GLS2 to be downregulated in $TSC2^{-/-}$ cells, suggesting it to be advantageous to these cells to limit the conversion of glutamine to glutamate.

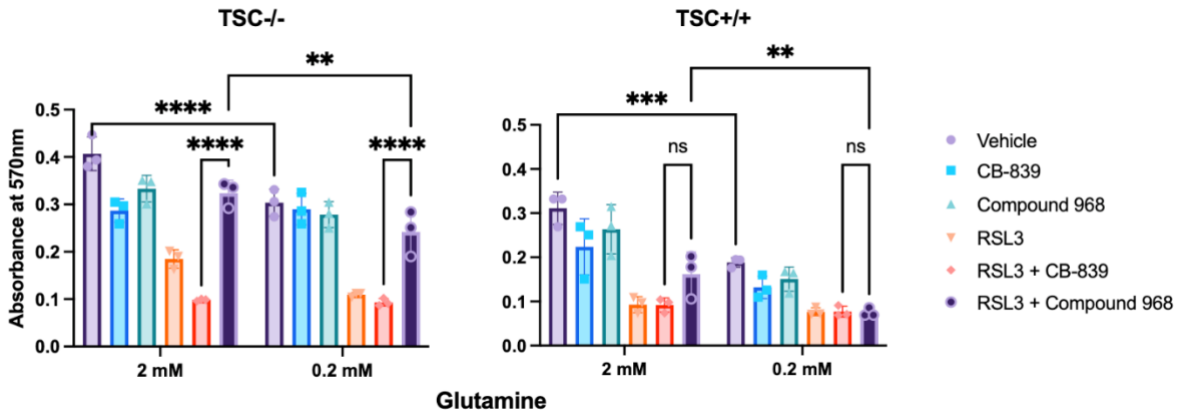

Figure 11: Effect of RSL3 (0.15uM) treatment following either compound 968 (10 µM) or CB-839 (10 µM) pre-treatment, in normal glutamine and glutamine-reduced media. Absorbance measurements were produced using MTT assay after 24 hours of incubation. Data is presented as mean values from three independent cell passage experiments, with the standard error of the mean (SEM) indicated by error bars. Statistical analysis was performed via Two-Way ANOVA, followed by Tukey's post-hoc test for multiple comparisons.

3.5 Glutaminase inhibitors and ferroptosis inducers do not influence extracellular glutamate concentration

Glutaminase enzymes convert glutamine to glutamate intracellularly to be used as a carbon source in the TCA cycle; furthermore, glutamate can also be exported by the antiporter System x_c^- to bring cystine into the cell as part of antioxidant defence mechanisms against ferroptosis. Glutamate used as a carbon source can contribute to the induction of ferroptosis through the production of reactive oxygen species as part of the ETC, that lead to lipid peroxidation. To investigate whether these mechanisms play a role in the vulnerabilty of $TSC2^{-/-}$ cells, we used a glutamate assay to establish any changes in the extracellular glutamate concentration. No signficant differences in extracellular glutamate concentrations were found when treating cells with combinations of RSL3 and compound 968, both individually and in conjunction (Fig. 12). Erastin, a known inhibitor of System x_c^-, was also used as a reference point. These data suggest that the modulation of cell viability and function seen in our other investigations has little impact on the availability of glutamate in the cell.

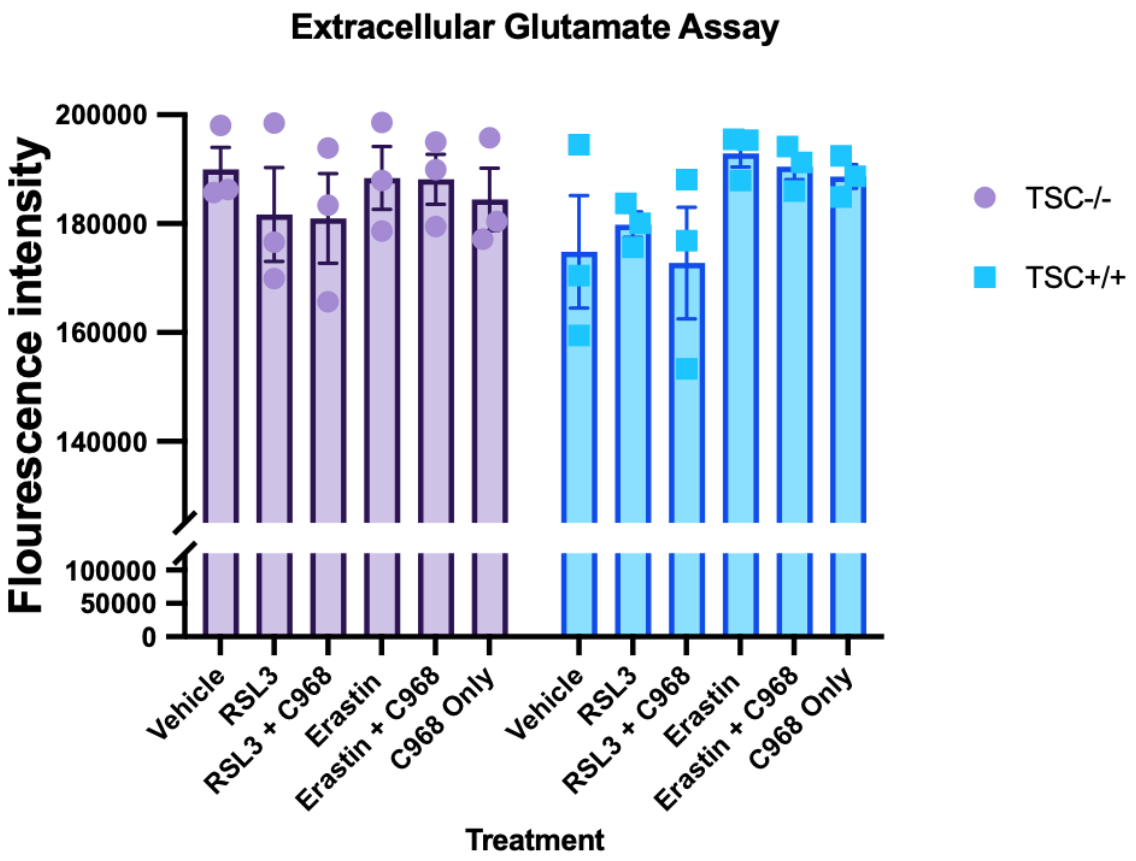

Figure 12: Changes in extracellular glutamate content of supernatant samples following exposure to ferroptosis inducing compounds and Compound 968. Erastin; 0.3 µM, RLS3; 0.15 µM; Compound 968; 10 µM. Data is presented as mean values from three independent cell passage experiments, with the standard error of the mean (SEM) indicated by error bars. Statistical analysis was performed via Two-Way ANOVA, followed by Dunnett's test to correct for multiple comparisons.

3.6 GLS2 knockout has little impact on the viability of $TSC2^{-/-}$ or $TSC2^{+/+}$ cells

The RNAseq analysis performed to compare the differences in RNA expression between $TSC2^{+/+}$ and $TSC2^{-/-}$ (Fig. 6) revealed that *GLS2* is downregulated in $TSC2^{-/-}$ cells. Artificially downregulating GLS2 via siRNA or CRISPR gene editing may lead to more similar cell phenotypes. Furthermore, as compound 968 is reported to inhibit both GLS1 and GLS2 (Lukey et al., 2019) whereas CB-839 targets GLS1 only, we used CRISPR-Cas9 gene editing to knockout *GLS2* from $TSC2^{-/-}$ and $TSC2^{+/+}$ cells (Fig. 13; Fig. 14) and subsequently observe the effects of these inhibitors on the altered cells.

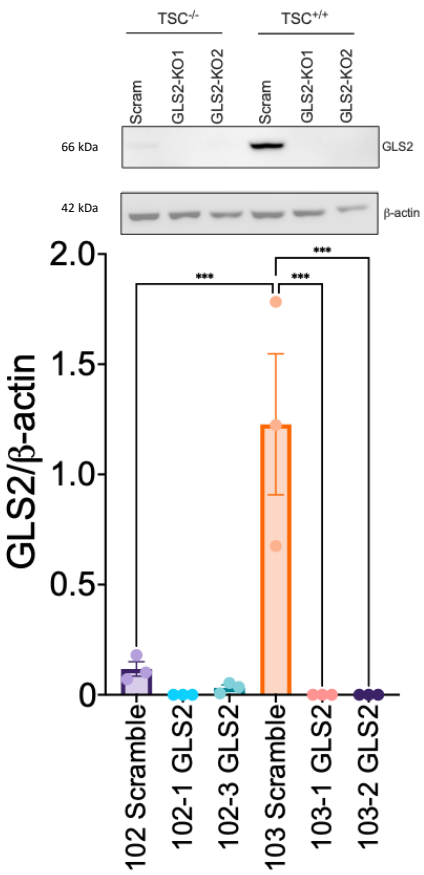

Figure 13: Western blot to confirm the successful knockout of GLS2 by CRISPR-Cas9 gene editing, and the differences in protein expression between the TSC2$^{-/-}$ and TSC2$^{+/+}$ cells at baseline. Y-axis represents the relative expression of GLS2 and common housekeeping protein β-actin.

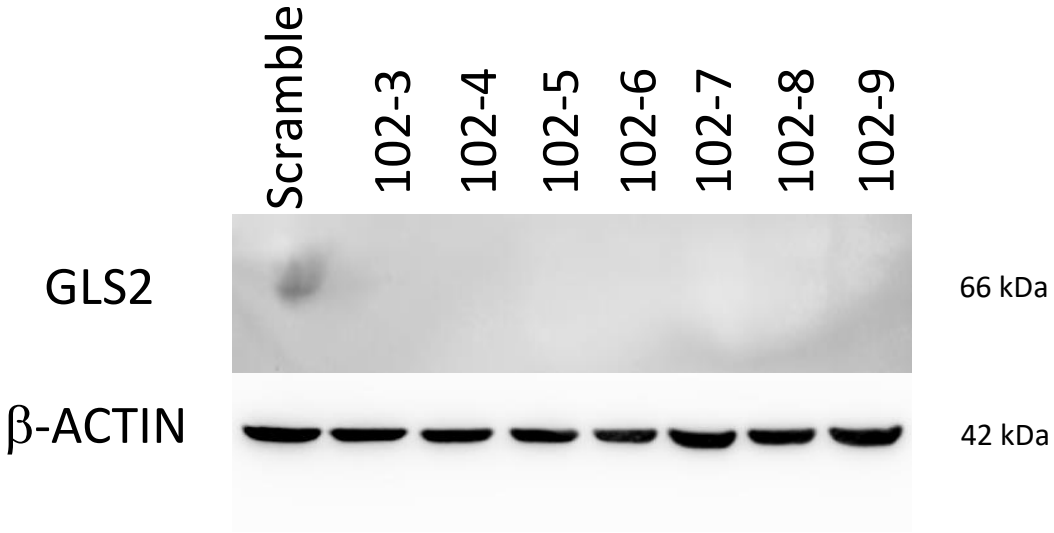

Figure 14: Western blot confirming the CRISPR knockout and baseline expression of GLS2 in TSC2$^{-/-}$ cells. '102-3' to '102-9' represent independent single cell clones following CRISPR-Cas9 transfection.

It can be seen in the results that ablation of GLS2 does not change the overall trend of results compared to the scrambled control cells (Fig. 8; Fig. 15). However, GLS2 knockout may have some impact on the degree of rescue experienced by $TSC2^{-/-}$ cells under Compound 968 treatment and does not have such an effect in comparable $TSC2^{+/+}$ cells. From this we can make two further predictions. Firstly, that GLS2 enzyme activity contributes to driving ferroptosis, as has been echoed in the RNA sequencing findings of section **3.1.** Additionally, we can suggest that the rescue effect experienced after treatment with Compound 968 is not due to its inhibition of GLS2, as the effect is still present even in the absence of the enzyme.

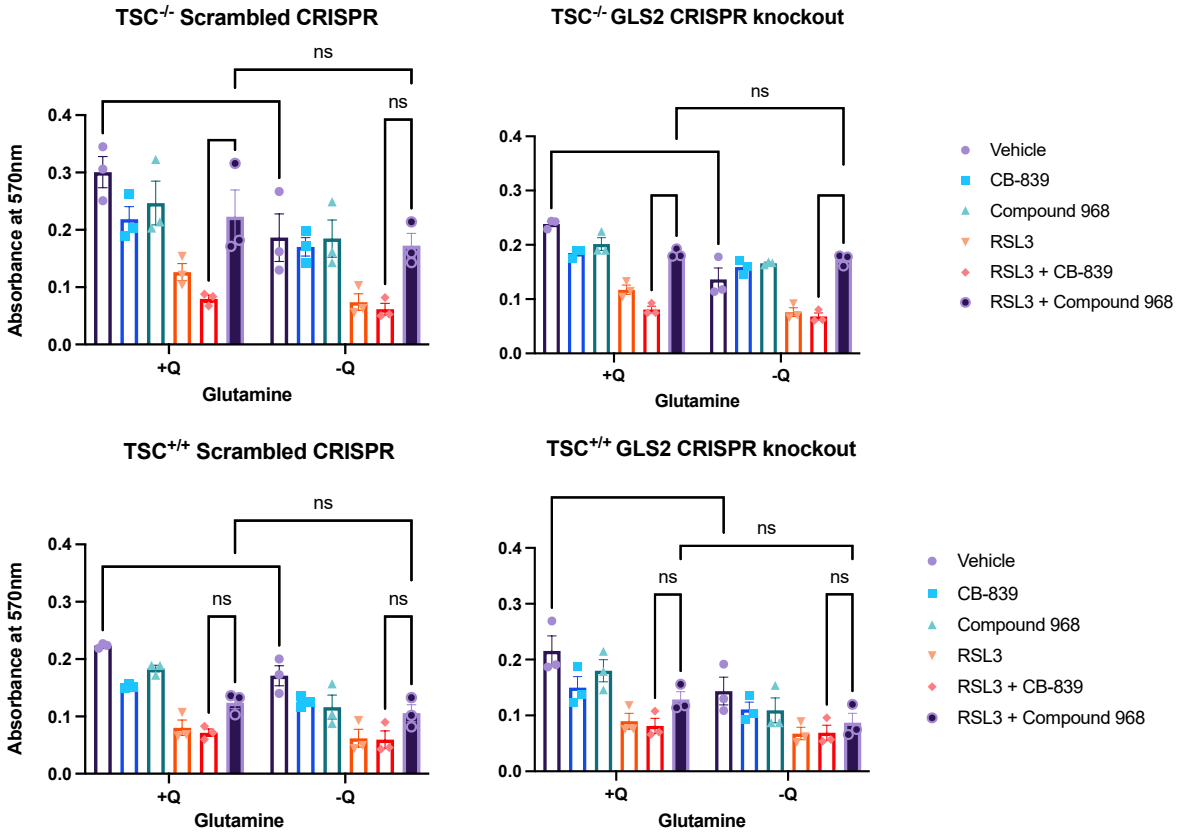

Figure 15: Effect of GLS2 knockout on the viability of $TSC^{-/-}$ and $TSC^{+/+}$ cells following treatment with ferroptosis inducer RSL3, and glutaminase inhibitors CB-839 and Compound 968. +Q = 2 mM, -Q = 0.2 mM. Absorbance measurements were produced using MTT assay after 24 hours of incubation. Clone 3 (102-3) as shown in figure 14 was used for these experiments. Data is presented as mean values from three independent cell passage experiments, with the standard error of the mean (SEM) indicated by error bars. Statistical analysis was performed via Two-Way ANOVA, followed by Tukey's post-hoc test for multiple comparisons.

3.7 GPX8 knockdown stimulates increased proliferation in $TSC2^{+/+}$ cells

As System X_c^- did not appear to be involved in the rescue from Compound 968 (Fig. 12), we next explored genes that are involved in cellular antioxidant systems, that may also depend on glutamine metabolism and the production of glutathione. Focusing on glutathione peroxidase enzymes, which rely on glutamine metabolism, RNA sequencing analysis undertaken on $TSC2^{-/-}$ and $TSC2^{+/+}$ cells identified *GPX8* (Fig. 6) as a gene of interest that is significantly upregulated in the $TSC2^{-/-}$ cells when compared to the $TSC2^{+/+}$ cells.

To identify possible mediators of the effects we have observed using Compound 968, we used short interfering RNA (siRNA) to knockdown *GPX8*. Whilst not statistically significant, a trend can be observed of increased absorbance between scrambled control and siGPX8 at all time points (Fig. 16). GPX8 has been shown to prevent the leakage of H_2O_2 from the endoplasmic reticulum (Ramming et al., 2014). H_2O_2 is a key radical species produced during mitochondrial respiration, that contributes to the accumulation of lipid peroxides that induce ferroptosis, reduction of which could enable more rapid proliferation. Unfortunately, for this data there is not confirmation of the level of knockdown induced by the siRNA.

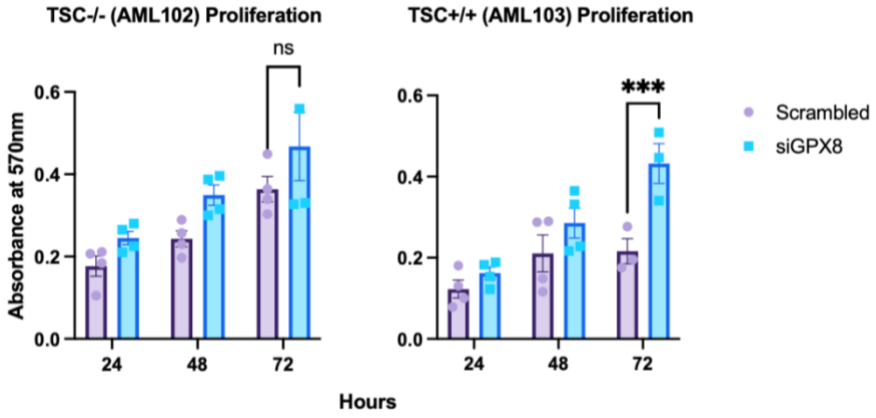

Figure 16: Effect of siGPX8 transfection on the rate of cell proliferation in $TSC2^{-/-}$ and $TSC2^{+/+}$ cells. Absorbance measurements were produced using MTT assay. Data is presented as mean values from at least three independent cell passage experiments, with the standard error of the mean (SEM) indicated by error bars. Statistical analysis was performed via Two-Way ANOVA.

3.8 Glutamine starvation may deplete expression of GPX8

Comparing $TSC2^{-/-}$ and $TSC2^{+/+}$ cells it was observed that $TSC2^{-/-}$ cells had a higher abundance of GPX8 (Fig. 6), which corresponds to the findings of the RNA sequencing analysis from section **3.1**. This could pin GPX8 as one factor behind the ability of $TSC2^{-/-}$ cells to rapidly proliferate, and their aggressive phenotype (Khatib et al., 2020). To begin to establish a link between GPX8, glutamine metabolism, and ferroptosis, we wanted to examine if glutamine availability had an influence on the expression of GPX8. We used western blotting to visualise the expression of GPX8, in media containing 2.0 mM glutamine or 0.2 mM glutamine, with or without glutaminase inhibitors and inducers for ferroptosis. It can be observed that glutamine starvation leads to reduced expression of GPX8 in both $TSC2^{-/-}$ and $TSC2^{+/+}$ samples, with the effect more pronounced in the $TSC2^{+/+}$ cells (Fig. 17). It was difficult to assess the effect of RSL3 on GPX8, as treatment reduced the expression of β-actin, suggesting cytotoxicity. Interestingly compound 968 did rescue β-actin expression in the presence of RSL3, suggesting GLS1/GLS2 may contribute to ferroptosis.

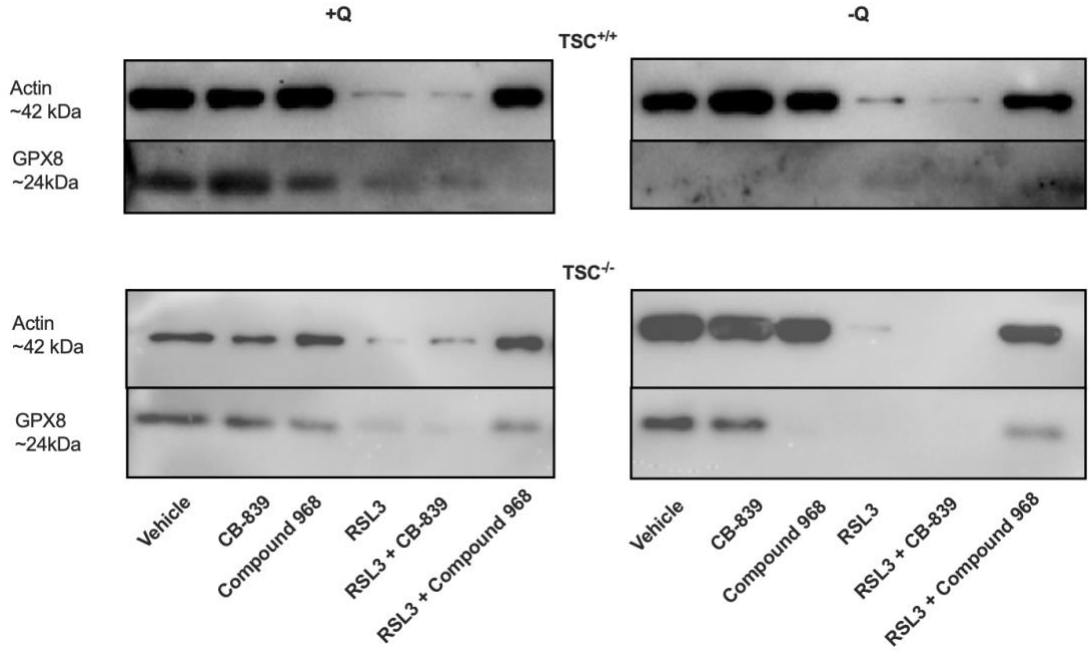

Figure 17: Western blot analysis of GPX8 expression in normal or starved glutamine conditions. Compound 968; 10 µM, CB-839; 10 µM, RSL3; 0.15 µM. Normal glutamine (+Q); 2 mM, starved glutamine (-Q); 0.2 mM.

3.9 Knockdown of GPX8 alters cell viability dependent upon the availability of glutamine

As reported previously, we wanted to establish the role of glutamine under both $TSC2^{-/-}$ cell viability and compound 968 mediated effects. Both $TSC2^{-/-}$ and $TSC2^{+/+}$ cells were transfected with siGPX8, and subsequently exposed to normal (2 mM) or starved (0.2 mM) while being treated with glutaminase inhibitors (CB-839 10 µM; Compound 968 10 µM) and RSL3 (0.15 µM). Viability was determined as absorbance measured by MTT assay. All experiments involved a 24-hour incubation period prior to measurement.

Results here show that *GPX8* knockdown had no overall effect on cell viability and did not have significant impacts on the effects of drug treatments (Fig. 18). $TSC2^{-/-}$ cells experienced rescue from RLS3 induced ferroptosis, following compound 968 treatment, in both the scrambled and siGPX8 samples. This observation does not differ between normal glutamine and glutamine starvation.

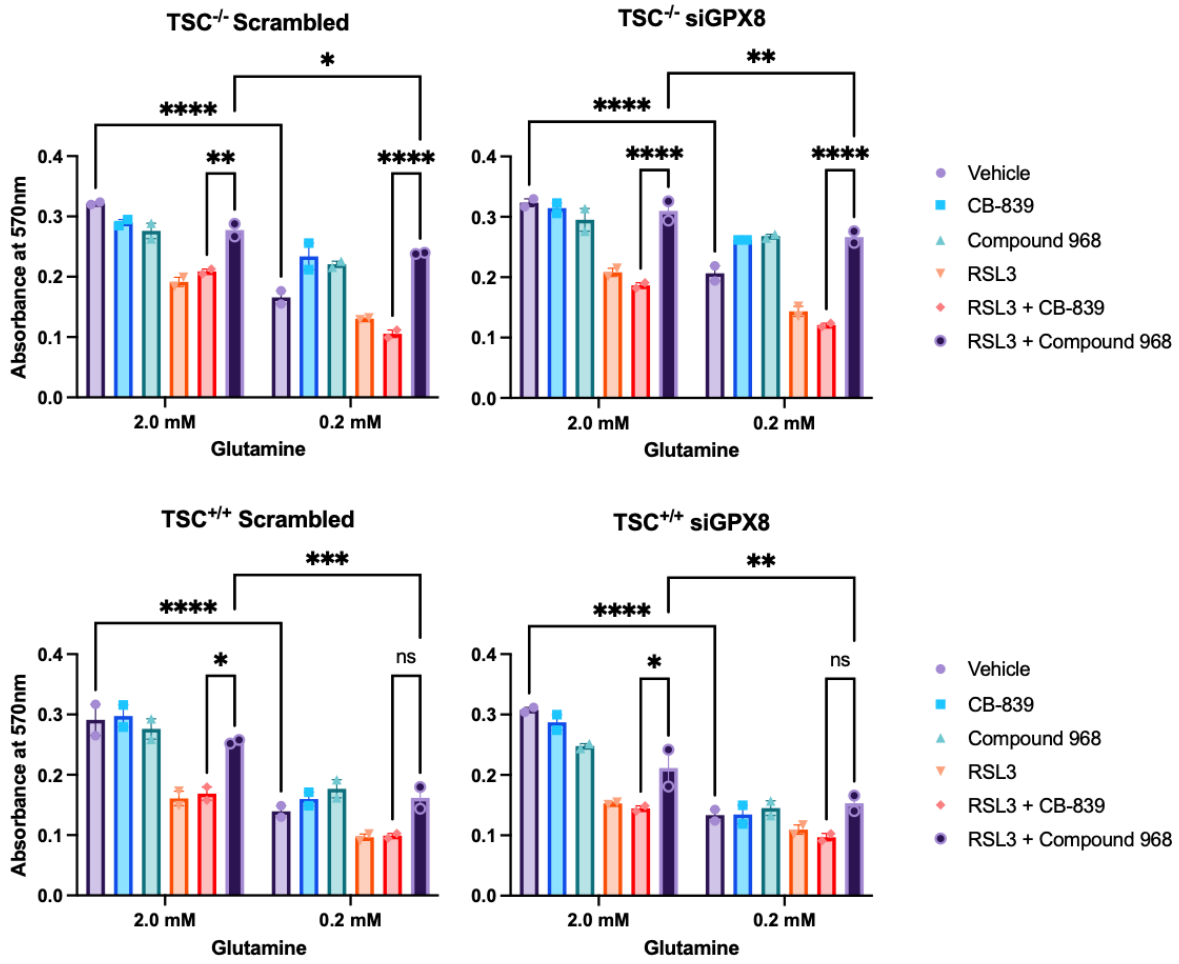

Figure 18: Effect of RSL3 (0.15 µM) treatment following either compound 968 (10 µM) or CB-839 (10 µM) pre-treatment, in normal glutamine and glutamine-reduced media. Treatments were carried out following siGPX8 transfection 72 hours prior. Absorbance measurements were produced using MTT assay after 24 hours of incubation. Data is presented as mean values from two independent cell passage experiments, with the standard error of the mean (SEM) indicated by error bars. Statistical analysis was performed via Two-Way ANOVA, followed by Tukey's post-hoc test for multiple comparisons.

3.10 GPX8 knockdown influences rate of mitochondrial respiration

Our primary goal in assessing metabolism using the Seahorse Bioscience XFe96 system was to ensure that the results we were observing in our MTT assays were not exclusively due to significant changes in metabolic rate, as the MTT assay depends on metabolic activity of mitochondria.

We observed that GPX8 knockdown had little to no impact on oxygen consumption rate (OCR) in either scramble or GPX8 depleted $TSC2^{-/-}$; whereas depletion of GPX8 in $TSC2^{+/+}$ cells caused a robust increase in OCR compared to the scrambled control (Fig. 19). Interestingly, TRI103 cells with GPX8 knockdown display very similar results to both the scrambled and GPX8 knockdown TRI102 cells. This increase in oxygen consumption could be due to its use as part of the lipid peroxidation mechanism **(1.6)** that goes unchecked in the absence of GPX8.

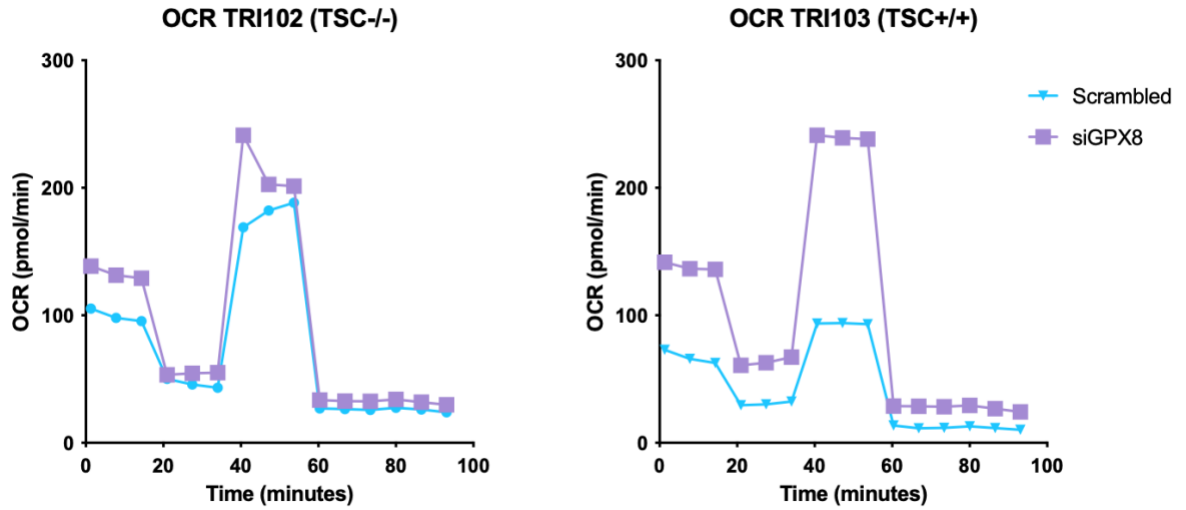

Figure 19: Effect of siGPX8 on oxygen consumption rate (OCR) in $TSC2^{-/-}$ and $TSC2^{+/+}$ cells, measured using the Seahorse Bioscience XFe96 analyser and associated mitochondrial stress test protocol. Four injections were used according to the stress test protocol: Oligomycin, FCCP, Rotenone/Antimycin A, and Monensin. Statistical analysis was unable to be performed due to lack of independent biological repeats.

3.11 GPX8 knockout enhances the effects of glutaminase inhibition by compound 968

To reinforce the findings of our experiments using siRNA, we proceeded to use CRISPR gene editing to perform complete knockouts of desired genes and their downstream proteins. We used the LONZA nucleofector (Section **2.7.2**) to transfect our cells with two RNP complexes aimed at knocking out GPX8. These cells were then cultured identically to a scrambled control. To verify that the GPX8 knockout was successful, we extracted protein lysates from cell samples and analysed these using western blotting. Both $TSC2^{-/-}$ and $TSC2^{+/+}$ cells showed a reduction in the expression of GPX8, prior to single cell cloning, suggesting that the knockout was successful (Fig. 20).

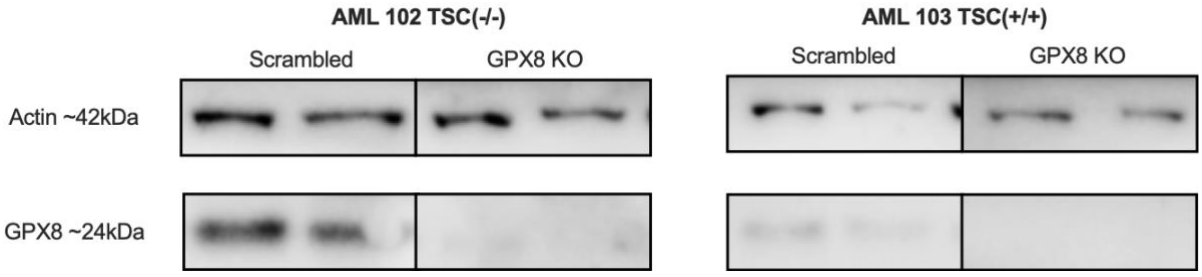

Figure 20: Western blot analysis for the knockout of GPX8 by CRISPR-Cas9. Two independent biological replicates were used to produce the matching bands.

CRISPR transfected cells were then treated similarly to previous experiments (**1.3, 1.4, 1.5**) with RSL3, CB-839, Compound 968, and normal or starved glutamine. In $TSC2^{-/-}$ cells, GPX8 knockout appears to enhance the rescue effect of Compound 968 for both normal and starved cells, with changes in p-value and changes in absolute significance respectively (Fig. 21). Importantly, these results follow the same pattern as previous experiments, showing that GPX8 knockdown or knockout is not fundamentally changing the nature of the cells response to glutamine or inducers of ferroptosis. In $TSC2^{+/+}$ cells, GPX8 knockout also enhanced compound 968 mediated rescue, but to a lesser degree. The effect was not significant in GPX8 knockout $TSC2^{+/+}$ cells under glutamine starvation (Fig. 21). It is not clear from these data what the consequence of GPX8 knockout is in this context but showing that Compound 968 mediated rescue was not altered in the relative absence of GPX8 enzyme action demonstrates that this is not the mode of action through which Compound 968 rescues cell viability.

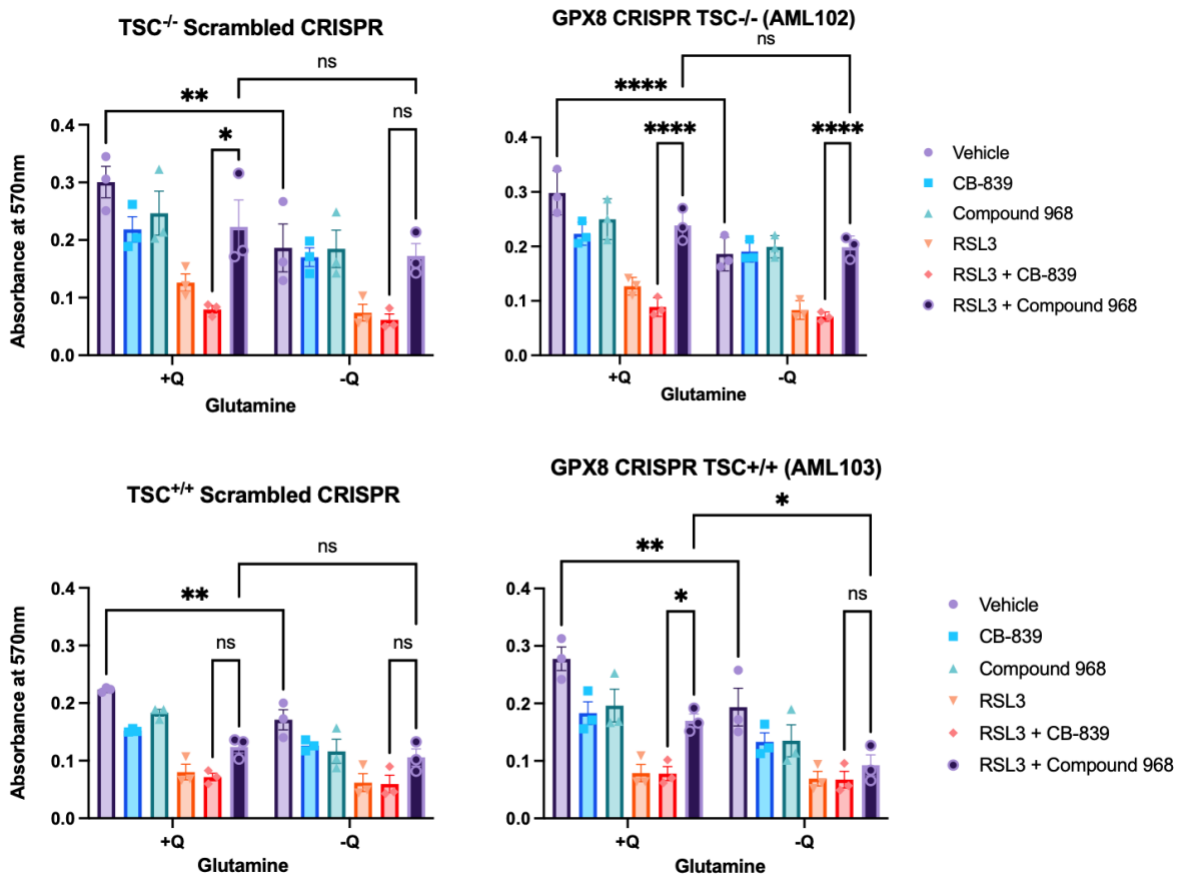

Figure 21: Effect of RSL3 (0.15 µM) treatment on scrambled or GPX8 knockout cells following CB-839 (10 µM) or Compound 968 (10 µM) pre-treatment, under normal or starved glutamine conditions. Absorbance measurements were produced using MTT assay after 24 hours of incubation. Data is presented as mean values from three independent cell passage experiments, with the standard error of the mean (SEM) indicated by error bars. Statistical analysis was performed via Two-Way ANOVA, followed by Tukey's post-hoc test for multiple comparisons.

3.12 GPX8 knockout may alter the phenotype of TSC2$^{-/-}$ but not TSC2$^{+/+}$ cells

For the scrambled control cells, the TSC2$^{-/-}$ cell line appeared to take on a more mesenchymal-like phenotype with slightly longer and more spindle-like cell shape. This is in keeping with the original derivation of these cells when it was first published (Yu et al., 2004; Hong et al., 2008). No changes could be observed in the TSC2$^{+/+}$ cells after knockout (Fig. 22; Fig. 23).

For single cell clone images, the transfected mix was serially diluted using the method described (**2.7.3**) and the same imaging protocol was then carried out.

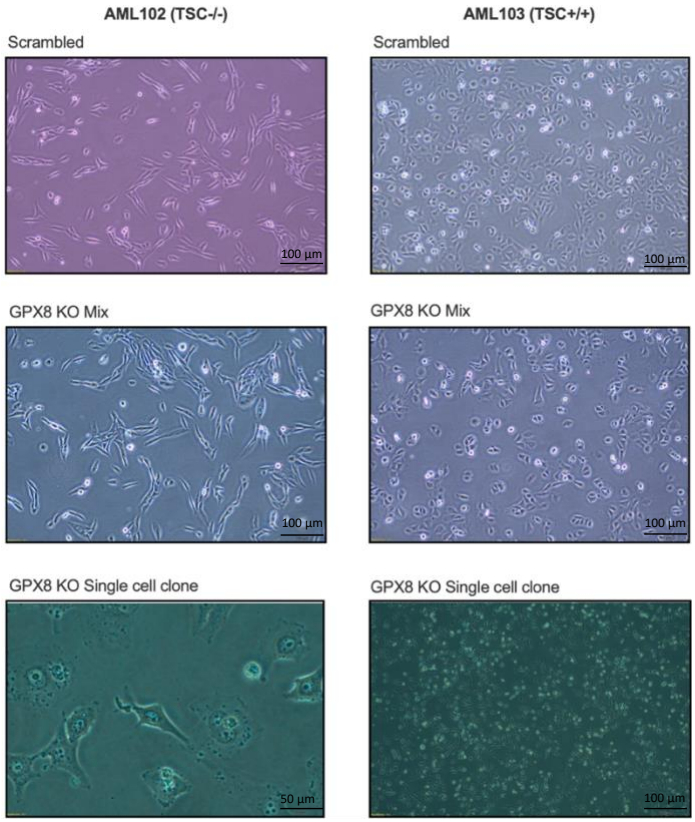

Figure 22: Images taken of culture cells following CRISPR knockout of GPX8. 'GPX8 KO Single cell clone' image taken at 40x magnification. All other images produced using 20x magnification.

3.13 Knockdown of SCD influences cell viability

Another gene of interest regarding TSC disease was stearoyl-CoA Desaturase (SCD), due to its link to ferroptosis as described in section 1.5.2. The SCD enzyme catalyses the production of monounsaturated fatty acids, that when incorporated into plasma membranes make them significantly less vulnerable to lipid peroxidation (Magtanong et al., 2019). TRI102 ($TSC2^{-/-}$) or TRI103 ($TSC2^{+/+}$) cells were depleted of *SCD* and treated with glutaminase inhibitors under different glutamine concentrations. Depletion of *SCD* reduced cell proliferation in TRI103 ($TSC2^{+/+}$), but not TRI102 ($TSC2^{-/-}$). Consistent with previous results, RSL3 reduced viability of both TRI102 ($TSC2^{-/-}$) and TRI103 ($TSC2^{+/+}$) cells. SCD knockdown had no significant effect on cell viability or on the rescue by Compound 968.

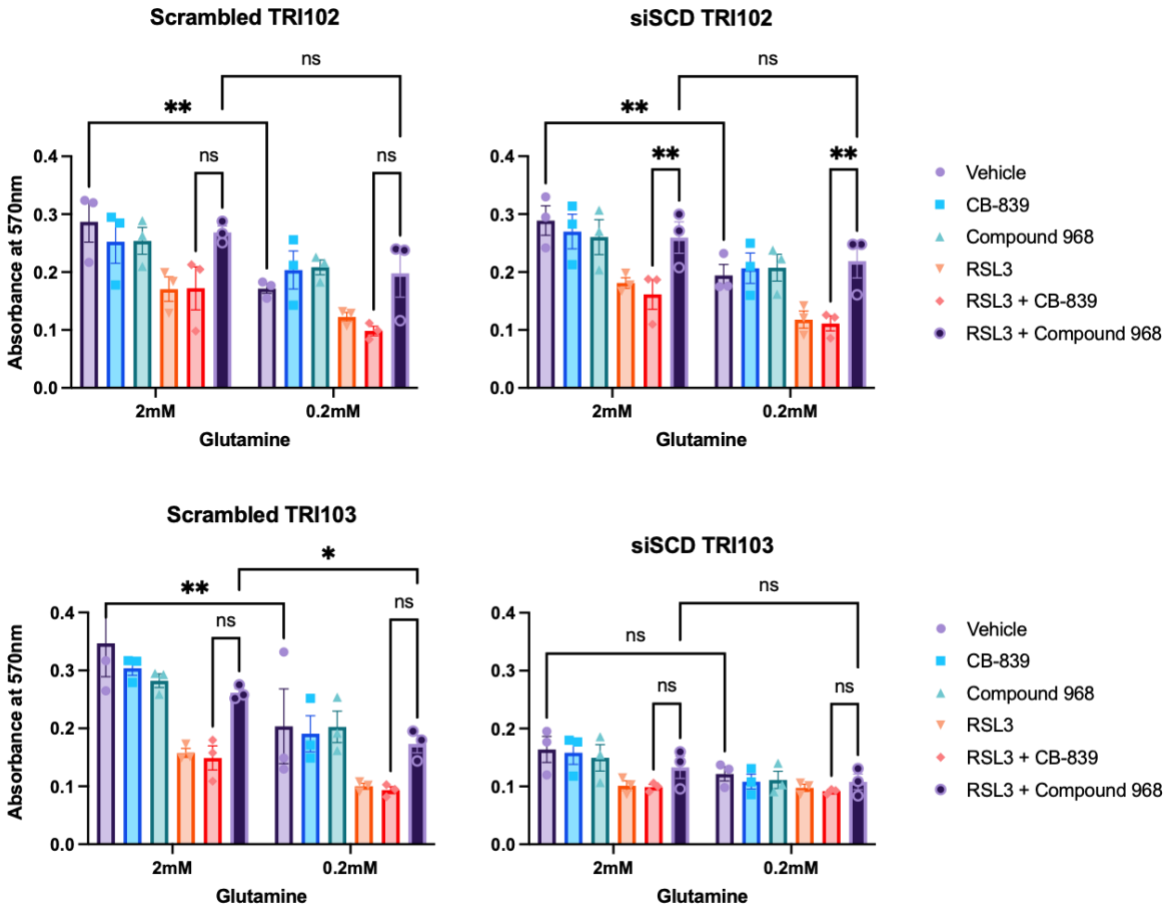

Figure 23: Effect of RSL3 (0.15 µM) treatment on scrambled and SCD knockdown cells following CB-839 (10 µM) or Compound 968 (10 µM) pre-treatment, under normal or starved glutamine conditions. Absorbance measurements were produced using MTT assay after 24 hours of incubation. Data is presented as mean values from three independent cell passage experiments, with the standard error of the mean (SEM) indicated by error bars. Statistical analysis was performed via Two-Way ANOVA, followed by Tukey's post-hoc test for multiple comparisons.

3.14 siSCD knockdown may influence rate of mitochondrial respiration

Using the Seahorse Bioscience XFe96 analyser we observed that siSCD knockdown may have some impact on oxygen consumption rate in $TSC2^{-/-}$ and $TSC2^{+/+}$ cells, with a greater degree of increase seen in $TSC2^{+/+}$ cells when compared to the scrambled baseline (Fig. 25). As the induction of ferroptosis relies on the production of reactive oxygen species by the electron transport chain, increased oxygen consumption could suggest an increase in radical species produced, and thus an increase in lipid peroxidation resulting in ferroptosis. We know that knockdown of SCD makes cells more vulnerable to ferroptosis (Tesfay et al., 2019), so these

findings could be further explored to evaluate the link between oxygen consumption and ferroptosis.

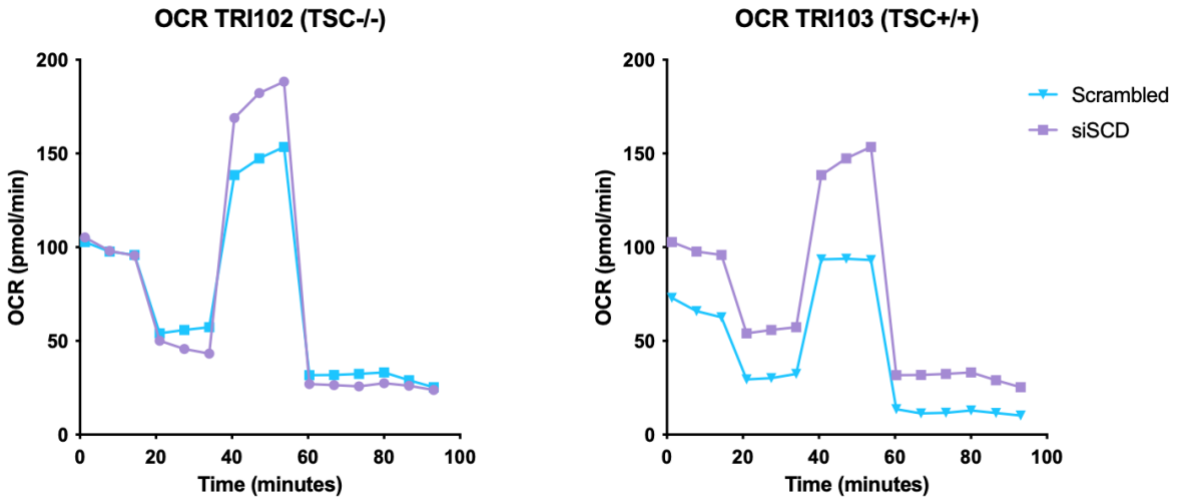

Figure 24: Effect of siSCD on oxygen consumption rate (OCR) in $TSC2^{-/-}$ and $TSC2^{+/+}$ cells, measured using the Seahorse Bioscience XFe96 analyser and associated mitochondrial stress test protocol. Four injections were used according to the stress test protocol: Oligomycin, FCCP, Rotenone/Antimycin A, and Monensin. Statistical analysis was not performed due to lack of independent biological repeats.

3.15 GPX8 and GLS2 knockout may alter the expression of TSC2

The TSC2 gene plays a central part in the induction of TSC disease, as it is one component of the TSC1/2 heterodimer that acts as a negative regulator of mTORC1. Therefore, altered expression of this gene is likely to have an impact on cell behaviour and the conclusions that can be drawn from our investigations. Cells lysates of CRISPR knockout clones and their scrambled equivalents were analysed using western blot to observe any possible effects on the expression of TSC2.

As expected, it can be seen that the expression of TSC2 in the $TSC2^{-/-}$ (TRI 102) cells is extremely low (Fig. 26). Furthermore, knockout of either GLS2 or GPX8 appears to very slightly restore TSC2 expression in these cells. As for the $TSC2^{+/+}$ (TRI 103) cells GLS2 knockout may slightly increase the expression of TSC2, while GPX8 knockout shows no clear effects.

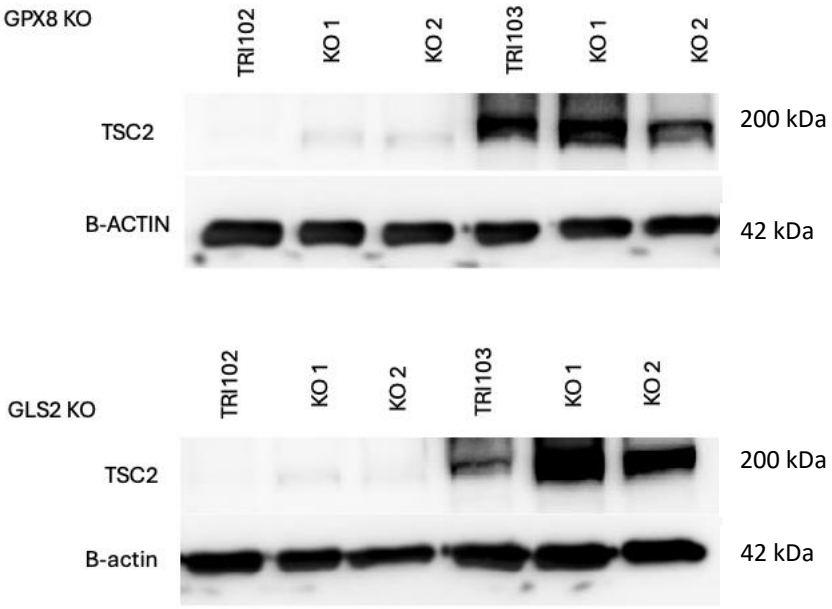

Figure 25: Western blots showing the expression of TSC2 following GPX8 or GLS2 knockout by CRISPR-Cas9 compared to scrambled controls. TRI103 – TSC2$^{+/+}$,TRI102 – TSC2$^{-/-}$.

4. Discussion

The wide range of tumours that present as a result of Tuberous Sclerosis Complex disease make conventional treatment especially challenging and enhance the need for a universal approach for this disease (Frost and Hulbert., 2015). Despite the enormous variety of possible clinical presentations in TSC disease, shared characteristics of diseased cells (and cancer in general) suggest a susceptibility to ferroptosis. This relatively novel form of programmed cell death remains under explored and provides a variety of avenues to be investigated.

This project aimed to unveil different mechanisms that could increase TSC cells susceptibility to ferroptosis, as well as understand ways that TSC2$^{-/-}$ cells are able to avoid death by ferroptosis. We hypothesised that the antioxidant enzyme GPX8 could play a key role in protecting TSC2$^{-/-}$ cells from ferroptosis. Furthermore, this theory extended to metabolic pre-requisites such as conversion of glutamine to glutamate, which could possibly be manipulated in a useful fashion.

4.1 Ferroptosis

Analysis of cell viability did not reveal any difference in susceptibility to ferroptosis between the two cell types, $TSC2^{+/+}$ and $TSC2^{-/-}$ (Fig. 8; 9; 10). This is opposite to what we would expect when considering the upregulation of key antioxidant proteins such as GPX8 and SLC7A11 in TRI102 $TSC2^{-/-}$cells (Fig. 6) that could assist in the evasion of ferroptosis. However, it does allow us to make stronger conclusions regarding any effectors of ferroptosis as we can be more certain that any changes in cell viability are down to experimental conditions, rather than cell phenotype. Moreover, this finding strongly distinguishes the roles of GPX4 and GPX8. GPX4, which is inhibited by RSL3, does not have significant differences in expression between $TSC2^{-/-}$ and $TSC2^{+/+}$ in the findings of our RNA sequencing analysis (Fig. 6). Therefore, while both proteins may play a role in antioxidant defence and the evasion of ferroptosis, their action on the cell is distinct.

Due to the increased rate of proliferation experienced by $TSC2^{-/-}$ cells due to lack of negative regulation of mTORC1 (Huang and Manning., 2008), there is an increased production of reactive oxygen species that result in lipid peroxidation leading to ferroptosis. If $TSC2^{-/-}$ cells are to evade ferroptosis they must have an enhanced mechanism for neutralising these reactive oxygen species. The results from figure 8 show that this mechanism is not GPX4, as there is no difference in vulnerability between $TSC2^{-/-}$ and $TSC2^{+/+}$. Therefore, we can safely conclude that there must be other factors involved in the ability of $TSC2^{-/-}$ cells to maintain redox balance while undergoing intense growth and proliferation.

The enzyme GLS2 is downregulated in $TSC2^{-/-}$ (Fig. 6) suggesting an advantage to the cell in some form. This enzyme catalyses the conversion of glutamine to glutamate, a process that can contribute to both the induction and evasion of ferroptosis. GLS2 has been reported as both tumourigenic (Buczkowska et al., 2023) and as a tumour suppressor (Suzuki et al., 2022) emphasising the complex dynamics this enzyme has within the cell. This complexity, combined with our data, could lead us to believe that GLS2 has an influence on ferroptosis and TSC disease.

4.2 Glutaminase inhibition

Viability assays revealed that not all glutaminase inhibition is created equal. In $TSC2^{-/-}$ cells, RSL3 induced cell death was significantly rescued, at all concentrations, by inhibition of GLS1/GLS2 with Compound 968 (Fig. 10). While in $TSC2^{+/+}$ cells, the rescue effect of Compound 968 was not statistically significant, but a slight trend can be seen (Fig. 10). In comparison, inhibition of GLS1 by CB-839 had no influence on the viability of the cells in either cell type (Fig. 9). This suggests that the rescue affect is brought about by the inhibition of GLS2. However, knockout of GLS2 using CRISPR-Cas9 did not result in the removal of this effect (Fig. 15). Therefore, our observations are independent of both reported targets of Compound 968 (GLS1/GLS2), leading us to investigate other avenues for the source of the viability rescue brought about by Compound 968.

Upregulation of GPX8 alongside downregulation of GLS2 could suggest that they have an influence on each other within the cell. However, western blot analysis revealed that inhibition of GLS1/GLS2 by CB-839 and Compound 968 alone does not have an impact on the expression of GPX8. Additional western blot analysis (Fig. 7) showed that GLS2 is expressed more highly in $TSC2^{+/+}$ cells compared to $TSC2^{-/-}$ cells, and that this relationship does not benefit TSC2 expression in a similar manner (Fig. 25) indicative of a possible inverse relationship between the functional TSC1/2 heterodimer and GLS2. Glutathione peroxidase enzymes are reliant on both glutamine (glutamine enzyme substrate) and glutamate (enzyme product) so it is likely that the enzymes may be linked in their roles in some respect. In establishing that Compound 968 can rescue cell viability independently of GLS1/GLS2 enzyme action, we must open the door to other methods of action for this inhibitor and its future research and pharmacological implications.

Western blot analysis of CRISPR-Cas9 knockouts of G*LS2* and *GPX8* showed that these genes may have an influence on the expression of TSC2 (Fig. 26). The implications of this finding are unclear, as increased expression of TSC2 alone may not lead to an increase in the functional TSC1/2 heterodimer. Nonetheless, the relationship between these genes is an interesting one and may link into further research on the topic.

4.3 Glutamine starvation

In addition to glutaminase enzyme inhibition, glutamine starvation was used to manipulate glutamine metabolism to investigate its effects on ferroptosis in TSC disease. We found that glutamine starvation at 10% of normal concentration (0.2 mM) did not have an influence on cell viability under any of the conditions subjected, in either $TSC2^{-/-}$ or $TSC2^{+/+}$ cells (Fig. 11).

In cancer, it would be expected that glutamine starvation would result in significant effects on proliferation and metabolism (Spada et al., 2023; Jiang et al., 2019) due to the hallmark of increased utilization of and dependency on glutamine for cancer cell growth and survival. Therefore, it is unsurprising that when comparing the viability of the cells within each type both with and without glutamine starvation, there is a statistically significant decrease in cell viability (Fig. 11; 18; 21). However, the observation that glutamine starvation does not have a noticeable impact on the rescue effect of Compound 968 following ferroptosis by RSL3 (Fig. 10) raises interesting questions as to the mechanism behind the effects of Compound 968.

Due to the reliance of the glutathione peroxidase enzyme family on glutamine (Fig. 2), it is not surprising that glutamine starvation may lead to a decrease in GPX8 protein expression (Fig. 17)(Cruzat et al., 2021). However, our data shows that glutamine starvation did not have significant effects on cell viability in either cell type ($TSC2^{-/-}$ or $TSC2^{+/+}$) and draws interesting questions as to why GPX8 is upregulated in $TSC2^{-/-}$ cells, as per the RNA sequencing data (Fig. 6). Research published in the journal PNAS demonstrates GPX8 as a regulator of cancer aggressiveness (Khatib et al., 2020) while more recent research points to a relationship between GPX8 and the tumour immune microenvironment. Other research has also associated GPX8 with poor prognosis in gastric and breast cancer (Ren et al., 2022). A substantial link between TSC disease and GPX8 has not been established, but with the role of GPX8 in oxidative stress being further developed it will be interesting to follow how this changes in the future.

Overall, it is surprising that manipulating glutamine concentration did not have a significant impact on the outcomes of our investigations. Cancer is known to be reliant on glutamine to enable rapid growth and proliferation, further suggesting that TSC disease may behave in a different manner.

4.4 Glutamate

As a result of glutaminase inhibition by Compound 968, we expected to observe changes in the concentration of extracellular glutamate. Contrary to predictions, we observed no statistically significant changes in extracellular glutamate concentration, as measured by fluorescence assay, between any experimental conditions in either cell type (Fig. 12). This suggests that the effects observed following Compound 968 treatment are not a result of reduced glutamate concentrations.

An explanation for this finding could be found in reduced glutamate dehydrogenase (GDH) activity caused by Compound 968 (Yuan et al., 2016). This study investigated the anti-proliferative effects of Compound 968 using an MTT assay, in a similar manner to this report, and used ELISA assays to quantify relative GDH activity. They found statistically significant decreases in relative GDH activity as compound 968 concentration was increased. Glutamate dehydrogenase is a key enzyme in enabling the use of glutamine as a carbon source in the TCA cycle and the subsequent production of ATP, and more importantly reactive oxygen species, as part of the ETC. Reduced GDH activity implies a reduction in anaplerosis and consequent respiration rate of the cell. Reduction of reactive oxygen species would therefore reduce the level of lipid peroxidation within the cell, and the incidence of ferroptosis. Downstream products of the TCA cycle have been shown to enhance ferroptosis (Liu et al., 2023) allowing us to speculate that by linking this previous research together, we may establish the role of Compound 968 in rescuing cell viability. Reduced GDH enzyme activity caused by Compound 968 treatment would lead to less α-KG entering the TCA cycle, and lower production of the downstream products of this cycle that enhance ferroptosis.

4.5 Glutathione Peroxidase 8

Following on from *RNA-seq* data that revealed GPX8 as an upregulated gene in $TSC2^{-/-}$ cells, we performed a range of genetic knockdowns and knockouts to observe the influence of GPX8 on the cells. Short interfering RNA (siRNA) was used to knockdown GPX8, while CRISPR-Cas9 transfection and selective single-cell cloning were used to isolate GPX8-negative cells.

Using western blotting to assess the expression of GPX8 (Fig. 7) we found that GPX8 has increased expression in $TSC2^{-/-}$ compared to $TSC2^{+/+}$. This matches the findings of the RNA

sequencing analysis (Fig. 6). Protein expression data such as this may provide the basis for conclusions on the effect of GPX8, such as with cancer aggressiveness (Khatib et al., 2020), prognosis, and oxidative stress (Chen et al., 2023).

4.5.1 Short interfering RNA knockdown

Compared to a scrambled baseline, we expected to see reduced proliferation at all time points in cells with GPX8 knockdown. In fact, the opposite was true. Knockdown of GPX8 resulted in a significant increase in cell proliferation compared to the scrambled control in $TSC2^{+/+}$ cells, but a non-significant increase in $TSC2^{-/-}$ cells, after 72 hours (Fig. 16). This may be caused by increased energy availability as the cell is diverted away from the process of epithelial-mesenchymal transition, which GPX8 is strongly implicated in (Khatib et al., 2020; Rosland et al., 2019).

However, our results show that GPX8 knockdown does not influence the intensity of rescue caused by Compound 968 in $TSC2^{-/-}$ cells. In $TSC2^{+/+}$ cells the rescue effect is not significant following siGPX8 transfection and glutamine starvation, but this may be due to a much lower baseline of cell viability (Fig. 18). These results suggest that the rescue observed following Compound 968 treatment is not facilitated by GPX8. This conclusion is mirrored in data produced using CRISPR-Cas9 gene editing to knockout GPX8 (Fig. 21), leading to further questions in to why GPX8 is upregulated in $TSC2^{-/-}$ (as in section **3.12**), and what its impacts could be on Tuberous Sclerosis Complex disease.

There is currently no literature linking GPX8 and Compound 968, so this could pose an interesting question for further research. Based on our data, Compound 968 may regulate the effects of GPX8, possibly due their shared factor of glutamine. Figure 17 shows that GPX8 expression may be reliant on glutamine, and Compound 968 inhibits the conversion of glutamine to glutamate via GLS1/GLS2, so has the potential to be beneficial to GPX8 expression. Analysis of GPX8 expression by western blotting shows no significant changes in expression when cells are treated with Compound 968, under either glutamine starved or normal glutamine conditions (Fig. 17). However, when cells had ferroptosis induced by RSL3, and treated with Compound 968, viability appears to be restored with the restoration of GPX8 expression. (Fig. 18).

Using *Seahorse* metabolic analysis, it was observed that the knockdown of GPX8 may alter the oxygen consumption rate of $TSC2^{+/+}$ cells, but not $TSC2^{-/-}$ cells (Fig. 19). This may be a result of the reduced control of reactive oxygen species production, specifically H_2O_2, that GPX8 is responsible for (Ramming et al., 2014). There is no explanation for the difference in effect between cell types, and little literature around the metabolic implications of GPX8 knockdown. Several studies link GPX8 knockdown to impaired tumour growth, possibly due the lack of reactive oxygen species control (Yang et al., 2022; Yin et al., 2022; Nguyen et al., 2023).

4.5.2 GPX8 Knockout using CRISPR-Cas9 gene editing

Following on from the results of GPX8 knockdown, we used CRISPR-Cas9 gene editing and selective cloning to produce GPX8 knockout strains of both $TSC2^{-/-}$ and $TSC2^{+/+}$ cells. This knockout did not clearly alter the phenotype of either cell line when observed under the microscope (Fig. 22). Further investigation is required to delve in to and confirm any phenotype changes from this knockout. After single cell isolation, both cell lines appear to form slightly more epithelial-like phenotypes, indicative of a move away from EMT as mentioned previously. Considering the link between TSC1/2 and EMT (Lu et al., 2019; Valianou et al., 2019), the conclusion could be drawn that GPX8 is linked in with the mechanism of these phenotypic changes. The scrambled strains of our cell lines suggest to us that, at least in this specific cell type, GPX8 may lead to a more mesenchymal phenotype.

Western blotting was used to confirm GPX8 knockout in our CRISPR-Cas9 edited cell lines. The analysis shows both cell lines successfully had GPX8 knocked out preventing the protein from being expressed (Fig. 7; 20). These western blot images also show the difference in GPX8 expression between our $TSC2^{-/-}$ and $TSC2^{+/+}$ cells lines prior to CRISPR transfection. Conversely, western blot analysis has shown that knockout of GPX8 by CRISPR-Cas9 may influence the expression of TSC2 (Fig. 26). It is difficult to draw a solid conclusion from this data due to the two-way relationship between the rates of expression (Fig 6; 26). However, it presents further questions into the role of GPX8 in cancer and whether the enzyme is strictly promotional or has a more complex relationship, as is often the case.

We also carried out similar viability assessments using MTT assay, matching previous experimental conditions. In $TSC2^{-/-}$ cells, GPX8 knockout did not affect the trend of the results we see following treatment with RSL3, CB-839, and Compound 968 (Fig. 21). This effect also occurs regardless of glutamine concentration (2 mM or 0.2 mM). It did however increase the statistical significance of the rescue effect seen with Compound 968 treatment. This matches up to our previous investigations using siGPX8 knockdown. Conversely, in $TSC2^{+/+}$, GPX8 knockout causes the ablation of the Compound 968 rescue effect at 0.2 mM glutamine, but the effect remains at 2 mM glutamine (Fig. 21).

The implications of these findings are unclear. Glutamine is not required for the catalytic activity of GPX8, as it is substituted for serine (Buday and Conrad., 2020; Toppo et al., 2008). The impact of Compound 968 treatment on cell viability suggests that glutamine plays a role in some way, but not as part of GPX8. The question then arises as to how these three elements are linked. GPX8 and glutamine have both been linked to calcium homeostasis (Nguyen et al., 2023; Moine et al., 2019) and lipid composition regulation (Nguyen et al., 2023; Cheng et al., 2023) so these could be important avenues of investigation in the future.

4.6 Glutaminase 2

Liver-type glutaminase 2 (GLS2) is one of the glutaminase enzymes and splice variants that is inhibited by Compound 968. In principle, inhibition of GLS2 should increase the concentration of glutamine in the cytoplasm, and decrease the concentration of glutamate, as the enzyme catalyses this conversion. In practice, there are far too many factors for it to be this simple. We found that Compound 968 does not have a significant effect on the concentration of extracellular glutamate in the supernatant of cultured cells (Fig. 12).

In experiments parallel to those for the knockout of GPX8, we also knocked out GLS2 from two separate $TSC2^{-/-}$ and $TSC2^{+/+}$ cell lines. Using MTT assays, we found that GLS2 knockout in $TSC2^{-/-}$ cells may enhance the rescue effects of Compound 968 after RSL3 treatment, whereas in $TSC2^{+/+}$ the rescue effect is diminished and becomes not statistically significant (Fig. 15). It is important to keep in mind that these effects can be modest, with the cells treated with both RSL3 and Compound 968 having their viability returned close to that of the vehicle - or compound 968 alone - baseline. This may suggest that the rescue effect of Compound 968 is

independent of GLS2, and may be reliant on another glutaminase enzyme, or another mechanism entirely. Interestingly, while Compound 968 is an GLS1/GLS2 inhibitor, research has shown that CB-839 only inhibits GLS1. Throughout the length of this project and under all the various experimental conditions, CB-839 failed to exhibit any significant effects on the viability of the cells (Fig. 9; 11; 15; 21). Contrary to this observation, CB-839 has undergone, and is currently undergoing, clinical trials investigating its efficacy against various cancers (Tannir et al., 2022; Wicker et al., 2021; Meric-Bernstam et al., 2016). Many of these clinical trials are using CB-839 in combination therapy with other compounds to establish their effectiveness. Therefore, our findings that CB-839 does not have any immediately apparent impact on cell viability may not paint the full picture. Further to this, it has been shown in that same study that CB-839 had significant anti-proliferative activity in triple negative breast cancer, but not against the T47D breast cancer cell line (Gross et al., 2014). The authors attribute this to several factors, most interestingly to us being the dependence on extracellular glutamine for growth. In $TSC2^{-/-}$ cells hyperactivity of mTORC1 leads to glutamine "addiction" due to the intense energy demands of the cell (Medvetz et al., 2015). This could suggest differences in behaviour between $TSC2^{-/-}$ cancers, and those unrelated to TSC disease, that has not yet been explored thoroughly.

The research published on the topic is conflicted on the role of glutaminase, especially GLS2, in cancer. There are studies that have similar findings to ours that the role of the GLS2 may be context dependent (Lukey et al., 2019; Hu et al., 2010; Suzuki et al., 2010), indicating that GLS2 can act as both a tumour suppressor and an onco-supportive enzyme. The inhibitor of GLS1, CB-839, has been shown to be effective antiproliferative agent against triple negative breast cancer (Gross et al., 2014). However, it has more recently undergone phase 2 clinical trials as a treatment for non-small cell lung cancer, but unfortunately failed to provide benefit compared to current immunotherapy options (Vasan and Chandel., 2024).

In our analysis of RNAseq data produced from TRI102 ($TSC2^{-/-}$) and TRI103 ($TSC2^{+/+}$) cells, we found that GLS2 was significantly downregulated in $TSC2^{-/-}$ (Fig. 6; 7). This indicates that there would be an increased availability of glutamine in $TSC2^{-/-}$ due to less being converted to glutamate. However, it also suggests that less glutamine is being used as a carbon source to produce ATP through the TCA cycle, which we know is a key to the maintenance of rapid

growth and proliferation in cancer (Plaitakis et al., 2017). Furthermore, there is likely to be a benefit to this downregulation. We suggest this is to enhance the amount of glutamine available or the synthesis and function of glutathione peroxidase enzymes, of which we have shown that GPX8 is at least somewhat dependent on glutamine for its expression (Fig. 8). Increased glutathione peroxidase expression helps to protect the cell from excessive production of reactive oxygen species that would lead to ferroptosis by lipid peroxidation.

Western blot analysis of GLS2 knockout cells by CRISPR-Cas9 added another layer to the results, showing that GLS2 knockout increases the expression of TSC2 in both $TSC2^{-/-}$ and $TSC2^{+/+}$ cells (Fig. 26). This evidence could suggest that GLS2 is acting here as a tumour promoter, inhibiting the expression of TSC2 to prevent the normal function of the TSC1/TSC2 heterodimer that acts as a negative regulator of mTORC1.

4.7 Stearoyl-CoA 9-Desaturase

Stearoyl-CoA Desaturase is an enzyme that converts saturated fatty acids into monounsaturated fatty acids. Monounsaturated fatty acids are less susceptible to lipid peroxidation, a key factor in ferroptosis, than polyunsaturated fatty acids, thus SCD can provide an element of protection from this form of cell death.

In our investigations using SCD small interfering RNA (siSCD) we found that there were no significant differences between scrambled and siSCD cells in either $TSC2^{-/-}$ or $TSC2^{+/+}$ cells over 24 hours (Fig. 24). Following this, we performed MTT assays to assess these cells response to our treatments. We found that SCD knockdown consistently reduces the ability of the cells to proliferate in both $TSC2^{-/-}$ and $TSC2^{+/+}$, regardless of treatments used (Fig. 24) This finding tracks nicely with previously conducted research that showed that an increase in the expression of SCD1 is correlated with cancer aggressiveness and poor prognosis (Tracz-Gaszewska and Dobrzyn., 2019; Sen et al., 2023).

We also explored the influence of SCD on the metabolic activity of our cells using the Seahorse XFe96 system. We observed a decreased rate of oxygen consumption (OCR) in siSCD transfected cells compared to their scrambled counterparts in both $TSC2^{-/-}$ and $TSC2^{+/+}$ cells

(Fig. 25). This finding has been reciprocated by researchers who measured the oxygen consumption rate of cell expressing shRNA-targeting SCD1 (Luis et al., 2021).

From our data we could not draw any conclusions as to a link between SCD and TSC-derived cancer. However, research published in 2019 linked SCD deficiency to activation of an mTORC1-PGC1a axis that regulates ER stress (Aljohani et al., 2019). The TSC1/TSC2 heterodimer is the negative regulator of mTOR, and its dysfunction by mutation of either part of the dimer is the cause of rapid tumour growth in TSC disease, thus posing an interesting research question for the future to link SCD and mTOR.

5. Conclusion

In conclusion, there are variety of factors that could enable the ability of $TSC2^{-/-}$ cells to avoid death by ferroptosis, most likely in conjunction with each other. Glutamine metabolism and its downstream effects provides a promising avenue for investigation in future work. Some research has already begun to lay the foundation for this conclusion and the link between TSC disease and ferroptosis (Zhang et al., 2021; Luo et al., 2018). Addressing our initial hypothesis, I believe that we have shown there may be a link between differentially expressed genes *GLS2* and *GPX8* and the evasion of ferroptosis in Tuberous Sclerosis Complex disease. However, more evidence is required to establish the precise mechanisms behind these relationships.

Our findings confirm that disruption of glutamine metabolism may have promising results in the future, but more effort is required to identify the definitive cause of the observed effects. Furthermore, we have added to existing literature linking GPX8 to both ferroptosis and cancer aggressiveness. Establishing that Compound 968 treatment can rescue cells from death by ferroptosis, but perhaps not through action on either GLS1 or GLS2, is an important finding and should encourage further investigation into this small molecule inhibitor.

Ferroptosis is a relatively young area of research, first being characterised in 2012 and alongside Tuberous Sclerosis Complex disease, they represent niche areas of investigation that have the potential to have significant impact on clinical practice in the future. We believe that increased understanding of the role of ferroptosis in TSC disease, including the elements explored in this thesis (SCD, GPX8, and glutamine metabolism), may enable improved care of

these individuals, as well as improving our broad understanding of the characteristics that are shared among cancer as a whole.

References

Ackermann, T., Shokry, E., Deshmukh, R., Anand, J., Galbraith, L. C., Mitchell, L., ... & Tardito, S. (2023). Paracrine secretion of MUFAs prevents ferroptosis in triple-negative breast cancer and reveals selenocysteine synthesis dependency for lung metastasis. bioRxiv, 2023-06. https://doi.org/10.1101/2023.06.13.544588

Aljohani, A., Khan, M. I., Syed, D. N., Abram, B., Lewis, S., Neill, L. O., Mukhtar, H., & Ntambi, J. M. (2019). Hepatic Stearoyl-CoA desaturase-1 deficiency-mediated activation of mTORC1- PGC-1α axis regulates ER stress during high-carbohydrate feeding. *Scientific reports*, *9*(1), 15761. https://doi.org/10.1038/s41598-019-52339-7

Amin, S., Lux, A., Calder, N., Laugharne, M., Osborne, J., & O'callaghan, F. (2017). Causes of mortality in individuals with tuberous sclerosis complex. Developmental medicine and child neurology, 59(6), 612–617. https://doi.org/10.1111/dmcn.13352

Arena, C., Bizzoca, M.E., Caponio, V.C., Troiano, G., Zhurakivska, K., Leuci, S., & Lo Muzio, L. (2021). Everolimus therapy and side-effects: A systematic review and meta-analysis. International Journal of Oncology, 59, 54. https://doi.org/10.3892/ijo.2021.5234

Ayala, A., Muñoz, M. F., & Argüelles, S. (2014). Lipid peroxidation: production, metabolism, and signaling mechanisms of malondialdehyde and 4-hydroxy-2-nonenal. Oxidative medicine and cellular longevity, 2014, 360438. https://doi.org/10.1155/2014/360438

Baba, Y., Higa, J. K., Shimada, B. K., Horiuchi, K. M., Suhara, T., Kobayashi, M., Woo, J. D., Aoyagi, H., Marh, K. S., Kitaoka, H., & Matsui, T. (2018). Protective effects of the mechanistic target of rapamycin against excess iron and ferroptosis in cardiomyocytes. American journal of physiology. Heart and circulatory physiology, 314(3), H659–H668. https://doi.org/10.1152/ajpheart.00452.2017

Battaglia, A. M., Chirillo, R., Aversa, I., Sacco, A., Costanzo, F., & Biamonte, F. (2020). Ferroptosis and Cancer: Mitochondria Meet the “Iron Maiden” Cell Death. *Cells*, *9*(6), 1505. https://doi.org/10.3390/cells9061505

Buczkowska, J., & Szeliga, M. (2023). Two Faces of Glutaminase GLS2 in Carcinogenesis. Cancers, 15(23), 5566. https://doi.org/10.3390/cancers15235566

Buday, K., & Conrad, M. (2020). Emerging roles for non-selenium containing ER-resident glutathione peroxidases in cell signaling and disease. *Biological chemistry*, *402*(3), 271–287. https://doi.org/10.1515/hsz-2020-0286

Champion, J. D., Dodd, K. M., Lam, H. C., Alzahrani, M. A., Seifan, S., Rad, E., ... & Tee, A. R. (2022). Drug inhibition of redox factor-1 restores hypoxia-driven changes in tuberous sclerosis complex 2 deficient cells. Cancers, 14(24), 6195; https://doi.org/10.3390/cancers14246195

Champion, Jesse 2023. Targeting the REF1/STAT3 axis to treat tuberous sclerosis. PhD Thesis, Cardiff University.

Chen, X., Yu, C., Kang, R., & Tang, D. (2020). Iron metabolism in ferroptosis. Frontiers in cell and developmental biology, 8, 590226. https://doi.org/10.3389/fcell.2020.590226

Chen, X., Yuan, L., Zhang, L., Chen, L., He, Y., Wang, C., ... & Yu, D. (2023). GPX8 deficiency–induced oxidative stress reprogrammed m6A epitranscriptome of oral cancer cells. Epigenetics, 18(1), 2208707.

Cheng, Y. J., Fan, F., Zhang, Z., & Zhang, H. jun. (2023). Lipid metabolism in malignant tumor brain metastasis: reprogramming and therapeutic potential. *Expert Opinion on Therapeutic Targets*, *27*(9), 861–878. https://doi.org/10.1080/14728222.2023.2255377

Conlon, M., Poltorack, C. D., Forcina, G. C., Armenta, D. A., Mallais, M., Perez, M. A., Wells, A., Kahanu, A., Magtanong, L., Watts, J. L., Pratt, D. A., & Dixon, S. J. (2021). A compendium of kinetic modulatory profiles identifies ferroptosis regulators. Nature chemical biology, 17(6), 665–674. https://doi.org/10.1038/s41589-021-00751-4

Cosialls, E., Pacreau, E., Duruel, C. et al. mTOR inhibition suppresses salinomycin-induced ferroptosis in breast cancer stem cells by ironing out mitochondrial dysfunctions. Cell Death Dis 14, 744 (2023). https://doi.org/10.1038/s41419-023-06262-5

Cruzat, V., Macedo Rogero, M., Noel Keane, K., Curi, R., & Newsholme, P. (2018). Glutamine: Metabolism and Immune Function, Supplementation and Clinical Translation. *Nutrients*, *10*(11), 1564. https://doi.org/10.3390/nu10111564

Darling, T. N., Pacheco–Rodriguez, G., Gorio, A., Lesma, E., Walker, C., & Moss, J. (2010). Lymphangioleiomyomatosis and TSC2-/- Cells. *Lymphatic Research and Biology*, *8*(1), 59–69. https://doi.org/10.1089/lrb.2009.0031

Dias, M. M., Adamoski, D., Dos Reis, L. M., Ascenção, C. F., de Oliveira, K. R., Mafra, A. C. P., ... & Dias, S. M. G. (2020). GLS2 is protumorigenic in breast cancers. Oncogene, 39(3), 690-702. https://doi.org/10.1038/s41388-019-1007-z

Dixon, S. J., Lemberg, K. M., Lamprecht, M. R., Skouta, R., Zaitsev, E. M., Gleason, C. E., ... & Stockwell, B. R. (2012). Ferroptosis: an iron-dependent form of nonapoptotic cell death. cell, 149(5), 1060-1072. https://doi.org/10.1016/j.cell.2012.03.042

Doll, S., Freitas, F. P., Shah, R., Aldrovandi, M., da Silva, M. C., Ingold, I., ... & Conrad, M. (2019). FSP1 is a glutathione-independent ferroptosis suppressor. Nature, 575(7784), 693-698.

Elmore S. (2007). Apoptosis: a review of programmed cell death. *Toxicologic pathology*, *35*(4), 495–516. https://doi.org/10.1080/01926230701320337

Evans, E. P. P., Scholten, J. T. M., Mzyk, A., Reyes-San-Martin, C., Llumbet, A. E., Hamoh, T., … Cantineau, A. E. P. (2021). Male subfertility and oxidative stress. *Redox Biology*, *46*, 102071. https://doi.org/10.1016/j.redox.2021.102071

Feng, H., & Stockwell, B. R. (2018). Unsolved mysteries: How does lipid peroxidation cause ferroptosis?. PLoS biology, 16(5), e2006203. https://doi.org/10.1371/journal.pbio.2006203

Flohé, L., & Brigelius-Flohé, R. (2011). Selenoproteins of the glutathione peroxidase family. In Selenium: Its Molecular Biology and Role in Human Health (pp. 167-180). New York, NY: Springer New York.

Flohé, L., Toppo, S., & Orian, L. (2022). The glutathione peroxidase family: Discoveries and mechanism. Free Radical Biology and Medicine, 187, 113-122. https://doi.org/10.1016/j.freeradbiomed.2022.05.003

Forcina, G. C., & Dixon, S. J. (2019). GPX4 at the crossroads of lipid homeostasis and ferroptosis. Proteomics, 19(18), 1800311. https://doi.org/10.1002/pmic.201800311

Frost, M., & Hulbert, J. (2015). Clinical management of tuberous sclerosis complex over the lifetime of a patient. Pediatric health, medicine and therapeutics, 6, 139–146. https://doi.org/10.2147/PHMT.S67342

Gan, B. (2022). ACSL4, PUFA, and ferroptosis: new arsenal in anti-tumor immunity. Signal transduction and targeted therapy, 7(1), 128. https://doi.org/10.1038/s41392-022-01004-z

Gonçalves, A. F., Adlesic, M., Brandt, S., Hejhal, T., Harlander, S., Sommer, L., ... & Frew, I. J. (2017). Evidence of renal angiomyolipoma neoplastic stem cells arising from renal epithelial cells. Nature communications, 8(1), 1466.

Gross, M. I., Demo, S. D., Dennison, J. B., Chen, L., Chernov-Rogan, T., Goyal, B., Janes, J. R., Laidig, G. J., Lewis, E. R., Li, J., Mackinnon, A. L., Parlati, F., Rodriguez, M. L., Shwonek, P. J., Sjogren, E. B., Stanton, T. F., Wang, T., Yang, J., Zhao, F., & Bennett, M. K. (2014). Antitumor activity of the glutaminase inhibitor CB-839 in triple-negative breast cancer. Molecular cancer therapeutics, 13(4), 890–901. https://doi.org/10.1158/1535-7163.MCT-13-0870

Guo, H., Li, W., Pan, G., Wang, C., Li, D., Liu, N., Sheng, X., & Yuan, L. (2023). The Glutaminase Inhibitor Compound 968 Exhibits Potent In vitro and In vivo Anti-tumor Effects in Endometrial Cancer. Anti-cancer agents in medicinal chemistry, 23(2), 210–221. https://doi.org/10.2174/1871520622666220513163341

Guo, Z., & Yan, F. (2024). Targeting glutamate metabolism in chronic lung diseases. Clinical and Translational Discovery, 4(2), e294. https://doi.org/10.1002/ctd2.294

Han C, Liu Y, Dai R, Ismail N, Su W, Li B. Ferroptosis and Its Potential Role in Human Diseases. Front Pharmacol. 2020 Mar 17;11:239. doi: 10.3389/fphar.2020.00239. PMID: 32256352; PMCID: PMC7090218. doi: 10.3389/fphar.2020.00239

Hatano, T., Atsuta, M., Inaba, H., Endo, K., & Egawa, S. (2018). Effect of everolimus treatment for renal angiomyolipoma associated with tuberous sclerosis complex: an evaluation based on tumor density. International Journal of Clinical Oncology, 23, 547-552.

Henning, Y., Blind, U. S., Larafa, S., Matschke, J., & Fandrey, J. (2022). Hypoxia aggravates ferroptosis in RPE cells by promoting the Fenton reaction. Cell death & disease, 13(7), 662. https://doi.org/10.1038/s41419-022-05121-z

Herzig, S., & Shaw, R. J. (2018). AMPK: guardian of metabolism and mitochondrial homeostasis. Nature reviews. Molecular cell biology, 19(2), 121–135. https://doi.org/10.1038/nrm.2017.95

Hong, F., Larrea, M. D., Doughty, C., Kwiatkowski, D. J., Squillace, R., & Slingerland, J.M.(2008). mTOR-Raptor Binds and Activates SGK1 to Regulate p27 Phosphorylation. Molecular Cell, 30(6), 701–711. https://doi.org/10.1016/j.molcel.2008.04.027

Kumar P, Zadjali F, Yao Y, Bissler JJ. Renal cystic disease in tuberous sclerosis complex. Experimental Biology and Medicine. 2021;246(19):2111-2117. doi:10.1177/15353702211038378

Hu, W., Zhang, C., Wu, R., Sun, Y., Levine, A., & Feng, Z. (2010). Glutaminase 2, a novel p53 target gene regulating energy metabolism and antioxidant function. *Proceedings of the National Academy of Sciences of the United States of America*, *107*(16), 7455–7460. https://doi.org/10.1073/pnas.1001006107

Huang, J., & Manning, B. D. (2008). The TSC1-TSC2 complex: a molecular switchboard controlling cell growth. The Biochemical journal, 412(2), 179–190. https://doi.org/10.1042/BJ20080281

Jiang, J., Srivastava, S., & Zhang, J. (2019). Starve cancer cells of glutamine: break the spell or make a hungry monster?. *Cancers*, *11*(6), 804.

Jin, J., Byun, J. K., Choi, Y. K., & Park, K. G. (2023). Targeting glutamine metabolism as a therapeutic strategy for cancer. Experimental & Molecular Medicine, 55(4), 706-715. https://doi.org/10.1038/s12276-023-00971-9

Jorge, Joana1; Santiago, Hugo1; Constantino, Beatriz1; Costa, Maria Inês1; Lapa, Beatriz1; Alves, Raquel1; Gonçalves, Ana Cristina1; Sarmento-Ribeiro, Ana Bela1. PB1910: TELAGLENASTAT (CB-839) IN MONOTHERAPY AND IN COMBINATION WITH EPIGENETIC MODULATORS OR IBRUTINIB INDUCES CELL DEATH IN CHRONIC LYMPHOCYTIC LEUKEMIA CELLS. HemaSphere 7(S3):p e43395a0, August 2023. | DOI: 10.1097/01.HS9.0000974464.43395.a0

Jyotsana, N., Ta, K. T., & DelGiorno, K. E. (2022). The role of cystine/glutamate antiporter SLC7A11/xCT in the pathophysiology of cancer. Frontiers in Oncology, 12, 858462. https://doi.org/10.3389/fonc.2022.858462

Khatib, A., Solaimuthu, B., Ben Yosef, M., Abu Rmaileh, A., Tanna, M., Oren, G., Schlesinger Frisch, M., Axelrod, J. H., Lichtenstein, M., & Shaul, Y. D. (2020). The glutathione peroxidase 8 (GPX8)/IL-6/STAT3 axis is essential in maintaining an aggressive breast cancer phenotype. Proceedings of the National Academy of Sciences of the United States of America, 117(35), 21420–21431. https://doi.org/10.1073/pnas.2010275117

Kodama, M., Oshikawa, K., Shimizu, H., Yoshioka, S., Takahashi, M., Izumi, Y., ... & Nakayama, K. I. (2020). A shift in glutamine nitrogen metabolism contributes to the malignant progression of cancer. Nature communications, 11(1), 1320. https://doi.org/10.1038/s41467-020-15136-9

Koppula, P., Zhuang, L., & Gan, B. (2021). Cystine transporter SLC7A11/xCT in cancer: ferroptosis, nutrient dependency, and cancer therapy. Protein & cell, 12(8), 599–620. https://doi.org/10.1007/s13238-020-00789-5

Lars Devisscher, Samya Van Coillie, Hofmans, S., Dries Van Rompaey, Goossens, K., Eline Meul, … Koen Augustyns. (2018). Discovery of Novel, Drug-Like Ferroptosis Inhibitors with in Vivo Efficacy. *Journal of Medicinal Chemistry*, *61*(22), 1012610140. https://doi.org/10.1021/acs.jmedchem.8b01299

Lee, D. Y., Song, M. Y., & Kim, E. H. (2021). Role of oxidative stress and Nrf2/KEAP1 signaling in colorectal cancer: mechanisms and therapeutic perspectives with phytochemicals. Antioxidants, 10(5), 743. https://doi.org/10.3390/antiox10050743

Lei, G., Zhuang, L., & Gan, B. (2021). mTORC1 and ferroptosis: Regulatory mechanisms and therapeutic potential. BioEssays : news and reviews in molecular, cellular and developmental biology, 43(8), e2100093. https://doi.org/10.1002/bies.202100093

Luo, M., Wu, L., Zhang, K. et al. miR-137 regulates ferroptosis by targeting glutamine transporter SLC1A5 in melanoma. Cell Death Differ 25, 1457–1472 (2018). https://doi.org/10.1038/s41418-017-0053-8

Li, H., Lin, Y., Zhang, L., Zhao, J., & Li, P. (2022). Ferroptosis and its emerging roles in acute pancreatitis. *Chinese Medical Journal*, *135*(17), 2026–2034. https://doi.org/10.1097/cm9.0000000000002096

Li, J., Cao, F., Yin, H. L., Huang, Z. J., Lin, Z. T., Mao, N., ... & Wang, G. (2020). Ferroptosis: past, present and future. Cell death & disease, 11(2), 88. https://doi.org/10.1038/s41419-020-2298-2

Li, M., Zhou, Y., Chen, C., Yang, T., Zhou, S., Chen, S., ... & Cui, Y. (2019). Efficacy and safety of mTOR inhibitors (rapamycin and its analogues) for tuberous sclerosis complex: a meta-analysis. Orphanet Journal of Rare Diseases, 14, 1-9. https://doi.org/10.1186/s13023-019-1012-x

Li, S., Jiang, X., Guan, M., Zhang, Y., Cao, Y., & Zhang, L. (2022). The overexpression of GPX8 is correlated with poor prognosis in GBM patients. Frontiers in Genetics, 13, 898204.

Liu L, Lian N, Shi L, Hao Z, Chen K. Ferroptosis: Mechanism and connections with cutaneous diseases. Front Cell Dev Biol. 2023 Jan 4;10:1079548. doi: 10.3389/fcell.2022.1079548. PMID: 36684424; PMCID: PMC9846271.

Liu, J., & Ma, D. W. (2014). The role of n-3 polyunsaturated fatty acids in the prevention and treatment of breast cancer. nutrients, 6(11), 5184-5223. https://doi.org/10.3390/nu6115184

Lu, Q., Chen, Y. B., Yang, H., Wang, W. W., Li, C. C., Wang, L., ... & Yin, X. X. (2019). Inactivation of TSC1 promotes epithelial-mesenchymal transition of renal tubular epithelial cells in mouse diabetic nephropathy. *Acta Pharmacologica Sinica*, *40*(12), 1555-1567. https://doi.org/10.1038/s41401-019-0244-6

Luis, G., Godfroid, A., Nishiumi, S., Cimino, J., Blacher, S., Maquoi, E., Wery, C., Collignon, A., Longuespée, R., Montero-Ruiz, L., Dassoul, I., Maloujahmoum, N., Pottier, C., Mazzucchelli, G., Depauw, E., Bellahcène, A., Yoshida, M., Noel, A., & Sounni, N. E. (2021). Tumor resistance to ferroptosis driven by Stearoyl-CoA Desaturase-1 (SCD1) in cancer cells and Fatty Acid Biding Protein-4 (FABP4) in tumor microenvironment promote tumor recurrence. *Redox biology*, *43*, 102006. https://doi.org/10.1016/j.redox.2021.102006

Lukey, M. J., Cluntun, A. A., Katt, W. P., Lin, M. J., Druso, J. E., Ramachandran, S., Erickson, J. W., Le, H. H., Wang, Z. E., Blank, B., Greene, K. S., & Cerione, R. A. (2019). Liver-Type Glutaminase GLS2 Is a Druggable Metabolic Node in Luminal-Subtype Breast Cancer. *Cell reports*, *29*(1), 76–88.e7. https://doi.org/10.1016/j.celrep.2019.08.076

Magtanong, L., Ko, P. J., To, M., Cao, J. Y., Forcina, G. C., Tarangelo, A., Ward, C. C., Cho, K., Patti, G. J., Nomura, D. K., Olzmann, J. A., & Dixon, S. J. (2019). Exogenous Monounsaturated Fatty Acids Promote a Ferroptosis-Resistant Cell State. Cell chemical biology, 26(3), 420–432.e9. https://doi.org/10.1016/j.chembiol.2018.11.016

Mason, P., Liang, B., Li, L., Fremgen, T., Murphy, E., Quinn, A., Madden, S. L., Biemann, H. P., Wang, B., Cohen, A., Komarnitsky, S., Jancsics, K., Hirth, B., Cooper, C. G., Lee, E., Wilson, S., Krumbholz, R., Schmid, S., Xiang, Y., Booker, M., … Carter, K. (2012). SCD1 inhibition causes cancer cell death by depleting mono-unsaturated fatty acids. *PloS one*, *7*(3), e33823. https://doi.org/10.1371/journal.pone.0033823

McCormack, F. X., Inoue, Y., Moss, J., Singer, L. G., Strange, C., Nakata, K., Barker, A. F., Chapman, J. T., Brantly, M. L., Stocks, J. M., Brown, K. K., Lynch, J. P., 3rd, Goldberg, H. J., Young, L. R., Kinder, B. W., Downey, G. P., Sullivan, E. J., Colby, T. V., McKay, R. T., Cohen, M. M., MILES Trial Group (2011). Efficacy and safety of sirolimus in lymphangioleiomyomatosis. The New England journal of medicine, 364(17), 1595–1606. https://doi.org/10.1056/NEJMoa1100391

McDonald, N. M., Hyde, C., Choi, A. B., Gulsrud, A. C., Kasari, C., Nelson III, C. A., & Jeste, S. S. (2020). Improving developmental abilities in infants with tuberous sclerosis complex: a pilot behavioral intervention study. Infants & Young Children, 33(2), 108-118.

McIlwain DR, Berger T, Mak TW. Caspase functions in cell death and disease. Cold Spring Harb Perspect Biol. 2013 Apr 1;5(4):a008656. doi: 10.1101/cshperspect.a008656. Erratum in: Cold Spring Harb Perspect Biol. 2015 Apr 01;7(4):a026716. doi: 10.1101/cshperspect.a026716.

Medvetz, D., Priolo, C., & Henske, E. P. (2015). Therapeutic targeting of cellular metabolism in cells with hyperactive mTORC1: a paradigm shift. *Molecular cancer research : MCR*, *13*(1), 3–8. https://doi.org/10.1158/1541-7786.MCR-14-0343

Meric-Bernstam, F., Tannir, N. M., Mier, J. W., DeMichele, A., Telli, M. L., Fan, A. C., ... & Harding, J. J. (2016). Phase 1 study of CB-839, a small molecule inhibitor of glutaminase (GLS), alone and in combination with everolimus (E) in patients (pts) with renal cell cancer (RCC). https://doi.org/10.1200/JCO.2016.34.15_suppl.4568

MILLS G. C. (1957). Hemoglobin catabolism. I. Glutathione peroxidase, an erythrocyte enzyme which protects hemoglobin from oxidative breakdown. The Journal of biological chemistry, 229(1), 189–197.

Moine, L., Pérez, A., Maldonado, C., de Talamoni, N. T., & de Barboza, G. D. (2019). Glutamine protects both transcellular and paracellular pathways of chick intestinal calcium absorption under oxidant conditions. *Comparative Biochemistry and Physiology Part A: Molecular & Integrative Physiology*, *238*, 110553. https://doi.org/10.1016/j.cbpa.2019.110553

Mortensen, M. S., Ruiz, J., & Watts, J. L. (2023). Polyunsaturated Fatty Acids Drive Lipid Peroxidation during Ferroptosis. Cells, 12(5), 804. https://doi.org/10.3390/cells12050804

Moss, J., Avila, N. A., Barnes, P. M., Litzenberger, R. A., Bechtle, J., Brooks, P. G., Hedin, C. J., Hunsberger, S., & Kristof, A. S. (2001). Prevalence and clinical characteristics of lymphangioleiomyomatosis (LAM) in patients with tuberous sclerosis complex. *American journal of respiratory and critical care medicine*, *164*(4), 669–671. https://doi.org/10.1164/ajrccm.164.4.2101154

Nair, N., Chakraborty, R., Mahajan, Z., Sharma, A., Sethi, S. K., & Raina, R. (2020). Renal Manifestations of Tuberous Sclerosis Complex. Journal of kidney cancer and VHL, 7(3), 5–19. https://doi.org/10.15586/jkcvhl.2020.131

National Health Service, August 2021, https://www.nhs.uk/conditions/tuberous-sclerosis/

National Institute of Neurological Disorders and Stroke, 2023. https://www.ninds.nih.gov/health-information/disorders/tuberous-sclerosis-

complex#:~:text=Tuberous%20sclerosis%20complex%20(TSC)%2C,heart%2C%20kidneys%2C%20and%20skin.

Nguyen, T. T. M., Nguyen, T. H., Kim, H. S., Dao, T. T. P., Moon, Y., Seo, M., Kang, S., Mai, V. H., An, Y. J., Jung, C. R., Kim, J. M., & Park, S. (2023). GPX8 regulates clear cell renal cell carcinoma tumorigenesis through promoting lipogenesis by NNMT. *Journal of experimental & clinical cancer research : CR*, *42*(1), 42. https://doi.org/10.1186/s13046-023-02607-2

Pei, J., Pan, X., Wei, G., & Hua, Y. (2023). Research progress of glutathione peroxidase family (GPX) in redoxidation. Frontiers in pharmacology, 14, 1147414.

Pizzorno, J. (2014). Glutathione!. Integrative Medicine: A Clinician's Journal, 13(1), 8.

Plaitakis, A., Kalef-Ezra, E., Kotzamani, D., Zaganas, I., & Spanaki, C. (2017). The glutamate dehydrogenase pathway and its roles in cell and tissue biology in health and disease. Biology, 6(1), 11. https://doi.org/10.3390/biology6010011

Pope, L. E., & Dixon, S. (2022). The role of monounsaturated fatty acids in ferroptosis. The FASEB Journal, 36. https://doi.org/10.1096/fasebj.2022.36.S1.0R871

Ramming, T., Hansen, H. G., Nagata, K., Ellgaard, L., & Appenzeller-Herzog, C. (2014). GPx8 peroxidase prevents leakage of H2O2 from the endoplasmic reticulum. Free Radical Biology and Medicine, 70, 106-116. https://doi.org/10.1016/j.freeradbiomed.2014.01.018

Ren, Z., He, Y., Yang, Q., Guo, J., Huang, H., Li, B., Wang, D., Yang, Z., & Tian, X. (2022). A Comprehensive Analysis of the Glutathione Peroxidase 8 (GPX8) in Human Cancer. *Frontiers in oncology*, *12*, 812811.https://doi.org/10.3389/fonc.2022.812811

Revilla-López, E., Berastegui, C., Méndez, A. et al. Long-term results of sirolimus treatment in lymphangioleiomyomatosis: a single referral centre experience. Sci Rep 11, 10171 (2021). https://doi.org/10.1038/s41598-021-89562-0

Riess, J., Frankel, P., Massarelli, E., Nieva, J., Lai, W.-C. .V, M. Koczywas, … Paik, P. (2022). MA13.08 A Phase 1 Trial of Sapanisertib and Telaglenastat (CB-839) in Patients with Advanced NSCLC (NCI 10327): Results from Dose Escalation. *Journal of Thoracic Oncology*, *17*(9), S91–S92. https://doi.org/10.1016/j.jtho.2022.07.153

Rodencal, J., & Dixon, S. J. (2023). A tale of two lipids: Lipid unsaturation commands ferroptosis sensitivity. Proteomics, 23, e2100308. https://doi.org/10.1002/pmic.202100308

Røsland, G. V., Dyrstad, S. E., Tusubira, D., Helwa, R., Tan, T. Z., Lotsberg, M. L., ... & Tronstad, K. J. (2019). Epithelial to mesenchymal transition (EMT) is associated with attenuation of succinate dehydrogenase (SDH) in breast cancer through reduced expression of SDHC. *Cancer & Metabolism*, *7*, 1-18.

Rotruck, J. T. ., Pope, A. L., Ganther, H. E., Swanson, A. B., Hafeman, D. G., & Hoekstra, W. (1973). Selenium: biochemical role as a component of glutathione peroxidase. Science, 179(4073), 588-590.

Sato, M., Kusumi, R., Hamashima, S., Kobayashi, S., Sasaki, S., Komiyama, Y., Izumikawa, T., Conrad, M., Bannai, S., & Sato, H. (2018). The ferroptosis inducer erastin irreversibly inhibits system x_c- and synergizes with cisplatin to increase cisplatin's cytotoxicity in cancer cells. Scientific reports, 8(1), 968. https://doi.org/10.1038/s41598-018-19213-4

Sen, U., Coleman, C., & Sen, T. (2023). Stearoyl coenzyme A desaturase-1: multitasker in cancer, metabolism, and ferroptosis. *Trends in cancer*, *9*(6), 480–489. https://doi.org/10.1016/j.trecan.2023.03.003

Seyfried, T. N., & Shelton, L. M. (2010). Cancer as a metabolic disease. Nutrition & metabolism, 7, 1-22. https://doi.org/10.1186/1743-7075-7-7

Shan, K., Fu, G., Li, J., Qi, Y., Feng, N., Li, Y., & Chen, Y. Q. (2023). Cis-monounsaturated fatty acids inhibit ferroptosis through downregulation of transferrin receptor 1. Nutrition Research, 118, 29-40. https://doi.org/10.1016/j.nutres.2023.07.002

Shan, K., Fu, G., Li, J., Qi, Y., Feng, N., Li, Y., & Chen, Y. Q. (2023). Cis-monounsaturated fatty acids inhibit ferroptosis through downregulation of transferrin receptor 1. *Nutrition Research*, *118*, 29-40. https://doi.org/10.1016/j.nutres.2023.07.002

Shen, Y. A., Chen, C. L., Huang, Y. H., Evans, E. E., Cheng, C. C., Chuang, Y. J., Zhang, C., & Le, A. (2021). Inhibition of glutaminolysis in combination with other therapies to improve cancer treatment. Current opinion in chemical biology, 62, 64–81. https://doi.org/10.1016/j.cbpa.2021.01.006

Shen, Y., Zhang, Y., Li, W., Chen, K., Xiang, M., & Ma, H. (2021). Glutamine metabolism: from proliferating cells to cardiomyocytes. *Metabolism - Clinical and Experimental*, *121*. https://doi.org/10.1016/j.metabol.2021.154778

Shibata, Y., Yasui, H., Higashikawa, K., Miyamoto, N., & Kuge, Y. (2019). Erastin, a ferroptosis-inducing agent, sensitized cancer cells to X-ray irradiation via glutathione starvation in vitro and in vivo. PloS one, 14(12), e0225931.

Słowińska, M., Kotulska, K., Szymańska, S., Roberds, S. L., Fladrowski, C., & Jóźwiak, S. (2021). Approach to preventive epilepsy treatment in tuberous sclerosis complex and current clinical practice in 23 countries. Pediatric Neurology, 115, 21-27.

Song, X., & Long, D. (2020). Nrf2 and ferroptosis: a new research direction for neurodegenerative diseases. Frontiers in neuroscience, 14, 484266.

Spada, M., Piras, C., Diana, G., Leoni, V. P., Frau, D. V., Serreli, G., Simbula, G., Loi, R., Noto, A., Murgia, F., Caria, P., & Atzori, L. (2023). Glutamine Starvation Affects Cell Cycle, Oxidative Homeostasis and Metabolism in Colorectal Cancer Cells. *Antioxidants (Basel, Switzerland)*, *12*(3), 683. https://doi.org/10.3390/antiox12030683

Stockwell, B. R. (2022). Ferroptosis turns 10: Emerging mechanisms, physiological functions, and therapeutic applications. Cell, 185(14), 2401-2421. https://doi.org/10.1016/j.cell.2022.06.003

Stockwell, B. R., Angeli, J. P. F., Bayir, H., Bush, A. I., Conrad, M., Dixon, S. J., ... & Zhang, D. D. (2017). Ferroptosis: a regulated cell death nexus linking metabolism, redox biology, and disease. Cell, 171(2), 273-285. https://doi.org/10.1016/j.cell.2017.09.021

Suzuki, S., Tanaka, T., Poyurovsky, M. V., Nagano, H., Mayama, T., Ohkubo, S., Lokshin, M., Hosokawa, H., Nakayama, T., Suzuki, Y., Sugano, S., Sato, E., Nagao, T., Yokote, K., Tatsuno, I., & Prives, C. (2010). Phosphate-activated glutaminase (GLS2), a p53-inducible regulator of glutamine metabolism and reactive oxygen species. *Proceedings of the National Academy of Sciences of the United States of America*, *107*(16), 7461–7466. https://doi.org/10.1073/pnas.1002459107

Suzuki, S., Venkatesh, D., Kanda, H., Nakayama, A., Hosokawa, H., Lee, E., ... & Prives, C. (2022). GLS2 is a tumor suppressor and a regulator of ferroptosis in hepatocellular carcinoma. Cancer research, 82(18), 3209-3222. https://doi.org/10.1158/0008-5472.CAN-21-3914

Suzuki, T., Muramatsu, A., Saito, R., Iso, T., Shibata, T., Kuwata, K., ... & Yamamoto, M. (2019). Molecular mechanism of cellular oxidative stress sensing by Keap1. Cell reports, 28(3), 746-758.

Taguchi, K., & Yamamoto, M. (2017). The KEAP1–NRF2 system in cancer. Frontiers in oncology, 7, 85.

Tang, D., Chen, X., Kang, R., & Kroemer, G. (2021). Ferroptosis: molecular mechanisms and health implications. Cell research, 31(2), 107-125. https://doi.org/10.1038/s41422-020-00441-1

Tannir, N. M., Agarwal, N., Porta, C., Lawrence, N. J., Motzer, R., McGregor, B., Lee, R. J., Jain, R. K., Davis, N., Appleman, L. J., Goodman, O., Jr, Stadler, W. M., Gandhi, S., Geynisman, D. M., Iacovelli, R., Mellado, B., Sepúlveda Sánchez, J. M., Figlin, R., Powles, T., Akella, L., … Escudier, B. (2022). Efficacy and Safety of Telaglenastat Plus Cabozantinib vs Placebo Plus Cabozantinib in Patients With Advanced Renal Cell Carcinoma: The CANTATA Randomized Clinical Trial. *JAMA oncology*, *8*(10), 1411–1418. https://doi.org/10.1001/jamaoncol.2022.3511

Tehrani, F., Khosroshahi, N., Keihani Doust, Z., Dabiran, S., & Zarkesh, M. R. (2023). The Efficacy and Safety of Rapamycin in Children with Tuberous Sclerosis: A Cross-sectional Study. Iranian journal of child neurology, 17(2), 19–29. https://doi.org/10.22037/ijcn.v17i2.36243

Tesfay, L., Paul, B. T., Konstorum, A., Deng, Z., Cox, A. O., Lee, J., Furdui, C. M., Hegde, P., Torti, F. M., & Torti, S. V. (2019). Stearoyl-CoA Desaturase 1 Protects Ovarian Cancer Cells from Ferroptotic Cell Death. Cancer research, 79(20), 5355–5366. https://doi.org/10.1158/0008-5472.CAN-19-0369

Toppo, S., Vanin, S., Bosello, V., & Tosatto, S. C. (2008). Evolutionary and structural insights into the multifaceted glutathione peroxidase (Gpx) superfamily. *Antioxidants & redox signaling*, *10*(9), 1501–1514. https://doi.org/10.1089/ars.2008.2057

Tracz-Gaszewska, Z., & Dobrzyn, P. (2019). Stearoyl-CoA Desaturase 1 as a Therapeutic Target for the Treatment of Cancer. *Cancers*, *11*(7), 948. https://doi.org/10.3390/cancers11070948

Trelinska, J., Dachowska, I., Kotulska, K., Fendler, W., Jozwiak, S., & Mlynarski, W. (2015). Complications of mammalian target of rapamycin inhibitor anticancer treatment among patients with tuberous sclerosis complex are common and occasionally life-threatening. Anti-cancer drugs, 26(4), 437–442. https://doi.org/10.1097/CAD.0000000000000207

Turner, A., & McGIVAN, J. D. (2003). Glutaminase isoform expression in cell lines derived from human colorectal adenomas and carcinomas. Biochemical Journal, 370(2), 403-408. https://doi.org/10.1042/bj20021360

Valianou, M., Filippidou, N., Johnson, D. L., Vogel, P., Zhang, E. Y., Liu, X., Lu, Y., Yu, J. J., Bissler, J. J., & Astrinidis, A. (2019). Rapalog resistance is associated with mesenchymal-type changes in Tsc2-null cells. *Scientific reports*, *9*(1), 3015. https://doi.org/10.1038/s41598-019-39418-5

Vasan, K., & Chandel, N. S. (2024). Molecular and cellular mechanisms underlying the failure of mitochondrial metabolism drugs in cancer clinical trials. *The Journal of Clinical Investigation*, *134*(3).

von Krusenstiern, A. N., & Stockwell, B. R. (2023). Determining the role of peroxidation of subcellular lipid membranes. Nature Chemical Biology, 19, 674-675. https://doi.org/10.1038/s41589-022-01250-w

von Krusenstiern, A. N., Robson, R. N., Qian, N., Qiu, B., Hu, F., Reznik, E., ... & Stockwell, B. R. (2023). Identification of essential sites of lipid peroxidation in ferroptosis. Nature chemical biology, 19(6), 719-730. https://doi.org/10.1038/s41589-022-01249-3

Wicker, C. A., Hunt, B. G., Krishnan, S., Aziz, K., Parajuli, S., Palackdharry, S., Elaban, W. R., Wise-Draper, T. M., Mills, G. B., Waltz, S. E., & Takiar, V. (2021). Glutaminase inhibition with telaglenastat (CB-839) improves treatment response in combination with ionizing radiation in head and neck squamous cell carcinoma models. *Cancer letters*, *502*, 180–188. https://doi.org/10.1016/j.canlet.2020.12.038

Wu, Y. J., Hu, Z. L., Hu, S. D., Li, Y. X., Xing, X. W., Yang, Y., & Du, X. H. (2019). Glutamate dehydrogenase inhibits tumor growth in gastric cancer through the Notch signaling pathway. Cancer Biomarkers, 26(3), 303-312.

Xiang, L., Mou, J., Shao, B., Wei, Y., Liang, H., Takano, N., ... & Xie, G. (2019). Glutaminase 1 expression in colorectal cancer cells is induced by hypoxia and required for tumor growth, invasion, and metastatic colonization. Cell death & disease, 10(2), 40.

Xie, Y., Hou, W., Song, X., Yu, Y., Huang, J., Sun, X., ... & Tang, D. (2016). Ferroptosis: process and function. Cell Death & Differentiation, 23(3), 369-379. https://doi.org/10.1038/cdd.2015.158

Yang, W. S., SriRamaratnam, R., Welsch, M. E., Shimada, K., Skouta, R., Viswanathan, V. S., ... & Stockwell, B. R. (2014). Regulation of ferroptotic cancer cell death by GPX4. Cell, 156(1), 317-331. https://doi.org/10.1016/j.cell.2013.12.010

Yang, Z. S., Yang, Q., Sun, X. X., Xiong, K., Zhu, X. T., Wang, Y. C., Ren, Q. Y., Wu, G. H., Wang, S. M., Cao, X. Q., Yang, X. R., & Jiang, W. G. (2022). GPX8 as a Novel Prognostic Factor and Potential Therapeutic Target in Primary Glioma. *Journal of immunology research*, *2022*, 8025055. https://doi.org/10.1155/2022/8025055

Ye, L., Wen, X., Qin, J., Zhang, X., Wang, Y., Wang, Z., … He, W. (2024). Metabolism-regulated ferroptosis in cancer progression and therapy. *Cell Death and Disease*, *15*(3). https://doi.org/10.1038/s41419-024-06584-y

Yin, J. X., Yang, R. F., Li, S., Renshaw, A. O., Li, Y. L., Schultz, H. D., & Zimmerman, M. C. (2010). Mitochondria-produced superoxide mediates angiotensin II-induced inhibition of neuronal potassium current. American Journal of Physiology-Cell Physiology, 298(4), C857-C865. https://doi.org/10.1152/ajpcell.00313.2009

Yin, X., Zhang, P., Xia, N., Wu, S., Liu, B., Weng, L., & Shang, M. (2022). GPx8 regulates apoptosis and autophagy in esophageal squamous cell carcinoma through the IRE1/JNK pathway. *Cellular Signalling*, *93*, 110307. https://doi.org/10.1016/j.cellsig.2022.110307

Yoo, H. C., Yu, Y. C., Sung, Y., & Han, J. M. (2020). Glutamine reliance in cell metabolism. Experimental & molecular medicine, 52(9), 1496-1516. https://doi.org/10.1038/s12276-020-00504-8

Yu, J., Astrinidis, A., Howard, S., & Henske, E. P. (2004). Estradiol and tamoxifen stimulate LAM-associated angiomyolipoma cell growth and activate both genomic and nongenomic signaling pathways. American journal of physiology. Lung cellular and molecular physiology, 286(4), L694–L700. https://doi.org/10.1152/ajplung.00204.2003

Yu, M., Gai, C., Li, Z., Ding, D., Zheng, J., Zhang, W., Lv, S., & Li, W. (2019). Targeted exosome-encapsulated erastin induced ferroptosis in triple negative breast cancer cells. Cancer science, 110(10), 3173–3182. https://doi.org/10.1111/cas.14181

Yu, X., Long, Y. Crosstalk between cystine and glutathione is critical for the regulation of amino acid signaling pathways and ferroptosis. Sci Rep 6, 30033 (2016). https://doi.org/10.1038/srep30033

Yuan, L., Sheng, X., Clark, L. H., Zhang, L., Guo, H., Jones, H. M., Willson, A. K., Gehrig, P. A., Zhou, C., & Bae-Jump, V. L. (2016). Glutaminase inhibitor compound 968 inhibits cell proliferation and sensitizes paclitaxel in ovarian cancer. American journal of translational research, 8(10), 4265–4277.

Zacharias, D. P. M., Lima, M. M. R., Souza Jr, A. L., de Abranches Oliveira Santos, I. D., Enokiara, M., Michalany, N., & Curi, R. (2003). Human cutaneous melanoma expresses a significant phosphate-dependent glutaminase activity: A comparison with the surrounding skin of the same patient. Cell biochemistry and function, 21(1), 81-84. https://doi.org/10.1002/cbf.997

Zhang, C., Liu, J., Zhao, Y., Yue, X., Zhu, Y., Wang, X., Wu, H., Blanco, F., Li, S., Bhanot, G., Haffty, B. G., Hu, W., & Feng, Z. (2016). Glutaminase 2 is a novel negative regulator of small GTPase Rac1 and mediates p53 function in suppressing metastasis. *eLife*, *5*, e10727. https://doi.org/10.7554/eLife.10727

Zhang, J., Pavlova, N. N., & Thompson, C. B. (2017). Cancer cell metabolism: the essential role of the nonessential amino acid, glutamine. *The EMBO Journal*, *36*(10), 1302–1315. https://doi.org/10.15252/embj.201696151

Zhao, Y., Li, Y., Zhang, R., Wang, F., Wang, T., & Jiao, Y. (2020). The Role of Erastin in Ferroptosis and Its Prospects in Cancer Therapy. OncoTargets and therapy, 13, 5429–5441. https://doi.org/10.2147/OTT.S254995

Zheng, Y. H., Yang, J. J., Tang, P. J., Zhu, Y., Chen, Z., She, C., ... & Xu, X. Y. (2021). A novel Keap1 inhibitor iKeap1 activates Nrf2 signaling and ameliorates hydrogen peroxide-induced oxidative injury and apoptosis in osteoblasts. Cell Death & Disease, 12(7), 679.